Commission of the European Communities

APPLICATION OF WEATHER RADAR FOR THE ALLEVIATION OF THE EFFECTS OF CLIMATIC HAZARD

Final Report from the United Kingdom Component

Contract No. EV4C-0039-UK (H)

Natural Environment Research Council

Institute of Hydrology
Maclean Building
Crowmarsh Gifford
Wallingford
Oxon OX10 8BB
UK

1992/058

Executive Summary

This is the final report from the UK component of the CEC project entitled "Application of Weather Radar for the Alleviation of the effects of Climate Hazard". It is made up of contributions from three radar groups working in the UK: the Institute of Hydrology, the University of Lancaster Institute of Environmental and Biological Sciences and the University of Salford Water Resources Research Group. Section 2 presents a case study of the preprocessing and calibration of Hameldon Hill weather radar, in an area strongly affected by orographic influences, and is the work of the Lancaster radar group. The Institute of Hydrology is responsible for the sections concerned with the London Weather Radar case studies on radar calibration (Section 3) and local rainfall forecasting (Section 4), the radar grid-square model for flood forecasting (Section 5) and design applications of weather radar (Section 6). Finally, the contribution concerned with urban applications of weather radar (Section 7) is from the Salford Water Resources Research Group. A summary of the main conclusions arising from the project are presented in Section 8.

Participants

The members of the research groups working at the three centres contributing to this report are presented below together with acknowledgements for funding and collaboration.

(i) Institute of Hydrology

Robert J. Moore	Project coordinator and leader
David A. Jones	Statistician
Dawn S. Hotchkiss	Meteorologist/modeller (from 1990)
Bryony May	Meteorologist/modeller (to 1989)
Kevin B. Black	Systems analyst/programmer
Lisa Stewart	Hydrologist

Additional funding from NRA Thames Region, the Flood Protection Commission of the Ministry of Agriculture Fisheries and Food and the Department of Environment is acknowledged.

(ii) University of Lancaster

Academic staff -	Dr. V.K. Collinge (project leader); Prof. P.C. Young; Dr. J.F.R.McIlveen (adviser and then project leader).
Research staff -	C. Buxton (initial research assistant); E.J. Archibald (research assistant); C. Blakeley (technician).
Research students -	K.R. Brown; M.E. Lord; T. McCormick replaced by J.Thielen.

Parallel support during the currency of the above was received from the Natural Environmental Research Council and North West Water.

Dr. Collinge was project leader at Lancaster throughout this period until his sudden illness in May 1991. His work was disrupted and then terminated by increasing

incapacity, culminating in his untimely death in early August. In late August Dr J.F.R. McIlveen took over the running of most of the radar-rainfall work at Lancaster, with Professor P. C. Young taking the time series analysis he had previously shared with Dr. Collinge. Although much work on this project was well documented (as witness the following report), it is obvious that Dr. Collinge had he lived would have collated and completed the project to an extent which has proved impossible, despite the dedicated efforts of his research assistant Ewan Archibald. Nevertheless it is hoped that the Lancaster component of the report does justice to the project and through it to the memory of a dedicated scientist and respected colleague.

(iii) University of Salford

Academic staff -	Professor I.D. Cluckie (Project leader); Dr R. Barber, Dr. K.A. Tilford, Dr G.A. Shepherd (Honorary Visiting Research Fellow), Mr M. Baker.
Research staff -	Dr Dawei Han, Dr R. Norreys, Mr J. Yuan, Mr L. Zhang.
Research students -	Mr D. Viner, Mr O. Wedgewood, Mr J. Cox, Mr R. Griffith, Mr B. Austin, Mr J. Laureys, Mr A. Wild, Mr B. Abes, Dr M. Pessoa, Dr P.S. Yu.

Funding from North West Water, NRA Western Region, NRA Anglian Region, NRA North West Region, Meteorological Office, Science and Engineering Research Council and the National Environment Research Council is acknowledged.

Contents

1. Introduction

Climatic hazards such as floods and droughts caused by rainfall extremes can be of a highly localised nature. Only through the use of weather radar can continuous measurements in space, as well as time, be achieved to permit studies of the spatial variability of climatic hazard, and to develop techniques to lessen their impact.

This report addresses how weather radar can be better used in the alleviation of the effects of climatic hazard through research on three broad themes. The first is through developing improved *radar preprocessing and calibration* techniques aimed at making radar measurements of rainfall more accurate and reliable. Consideration is given to improved radar rainfall measurement in both areas of significant and modest relief through case studies using the Hameldon Hill radar in a hilly area of North West England (Section 2) and the London Weather radar in lowland South East England (Section 3).

The second research theme on *flow forecasting* is addressed initially through the development of a radar-based rainfall forecasting procedure (Section 4) which provides a means of achieving extended lead-time flow forecasts through forecasting the rainfall input to rainfall-runoff models. Section 5 considers how maximum use of spatial radar estimates of rainfall can be made in flood and low flow forecasting through the development of rainfall-runoff models configured on the radar grid-square. The use of weather radar in storm hazard assessment for design applications is addressed in Section 6.

Theme three, on *urban applications* of weather radar considers, in particular, the need for high resolution data in space and time over smaller scale urban areas, the use of radar data in urban drainage modelling and the need for new types of radar for urban applications (Section 7). Finally, conclusions arising out of the research project are set out in Section 8.

2. Weather Radar Preprocessing and Calibration: The Hameldon Hill Case Study

2.1 Introduction

The main aims of the Hameldon Hill Case Study were:

(i) to produce improved techniques for calibrating the Hameldon Hill weather radar for rainfall measurement and short-term rainfall forecasting for an area within 75 km of the radar, for both frontal and convective events; and

(ii) to explore the use of these techniques at longer range, up to 150 km.

The Study was undertaken at the University of Lancaster using data from the unmanned C-band radar (Plessey type 45C, 5.6 cm wavelength, 1° beam width) sited at Hameldon Hill, 400 m above sea level near Burnley in North West England (Fig. 2.1). Initial research was confined to an area of 60x80 km^2, covered by

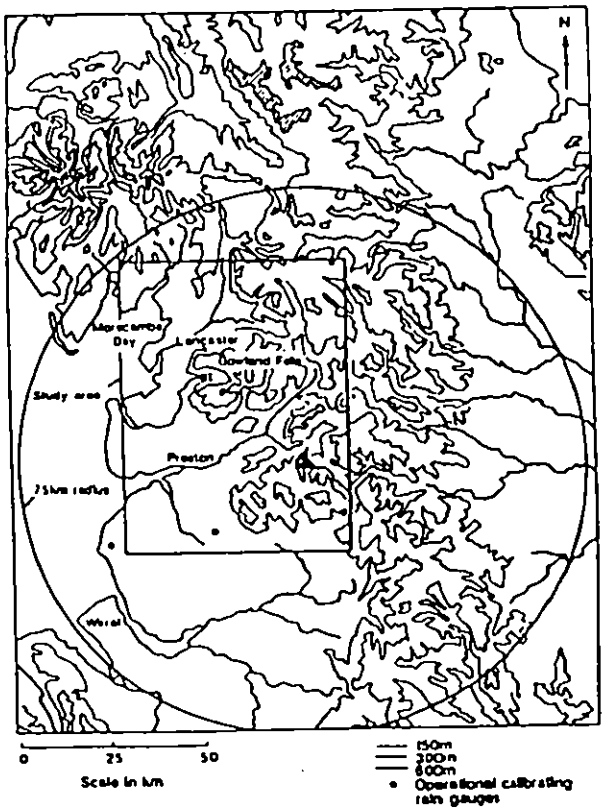

Figure 2.1 Location of Hameldon Hill radar in North West England

2x2 km² radar image pixels. This contained 28 recording raingauges (9 of them added by the University to those operated by the National Rivers Authority and the Meteorological Office), a coastal plain, and hills (the Bowland Fells) rising to 560 m. The study area was extended later to the full 75 km radius covered by 2x2 km² pixels, and containing 60 gauges and the Pennine and Lake District hills. Finally it was extended to the total land area within the full 200 km range covered by 5x5 km² pixels and containing about 1400 gauges. On the two smaller scales of study, careful scrutiny of recording raingauge date revealed frequent timing errors, requiring careful correction for case studies. Meteorological data were obtained from the University's weather station north west of the Bowland Fells, and from the Meteorological Office (including upper air data from Aughton, 50 km WSW of Hameldon Hill).

Much of the initial work was done in conditions of rain widespread over the study area, associated with a wide variety of meteorological conditions. Warm, cold and occluded fronts were usually involved. Most cases were chosen to avoid bright band conditions (estimated to affect Hameldon Hill half of the time), but some bright band cases were chosen for comparison (see 3.2 below). In the later stages, some cases of intense convective rainfall near Hameldon Hill were closely analysed, stimulating further study of radar observation of convective rain (see 3.5).

2.2 RADAR PREPROCESSING

The radar data used for the Study were supplied on magnetic tape by the United Kingdom Meteorological Office, and came from beam elevations of 0.5, 1.5, 2.5 and 4.0° at 5 minute intervals. Most data came from the lowest two of these beams, especially the 1.5° beam out to 24 km range, and the 0.5° beam beyond. On-site occultation correction, clutter cancellation, bright-band identification, conversion to 208 levels of rainfall rate, attenuation correction and conversion from polar to cartesian pixels (see 2.1 above) were included, but the final routine calibration using selected ground-truth gauges was removed by software written by the Meteorological Office. The data were restructured on the University's mainframe computer (VAX 1170, subsequently Sequent Symmetry) to be campatible with the visual, graphical display package "Rainfall Analysis Unit" from Software Sciences Ltd. Software was written to extract radar data from the four 2x2 km² pixels closest to each ground truth gauge and to calculate the "Assessment Factor", $AF = R_r/R_g$ from 15 minute, and longer totals of raingauge, R_g, and radar, R_r, data.

2.3. FACTORS AFFECTING THE RADAR-RAINGAUGE RELATIONSHIP

2.3.1 Orographic enhancement

All three areas of study around the Hameldon Hill radar data are likely to experience orographic enhancement of rainfall as moist westerly airstreams interact with the hilly terrain. Intensive study of the small area centred on the Bowland Fells, comparing radar data with the enlarged gauge network (Section 2.1), has shown orographic enhancement to be endemic and often substantial. Average annual rainfall on the highest ground is about 2000 mm, compared with 950 mm on the coastal plain to the west.

Radar data offers very complete coverage with adequate resolution (at least with $2km^2$ pixels), but is likely to miss some of the orographic enhancement when this is concentrated below beam level by the seeder-feeder mechanism, as will often be the case. A simple descriptive model was devised, with background rainfall growing linearly downward from zero 2.5 km above sea level and orographic enhancement of rainfall growing linearly downward from zero 1.5 km above ground level (after Hill et al 1981) to a maximum value at the ground surface (Fig. 2.2). If P_o is the

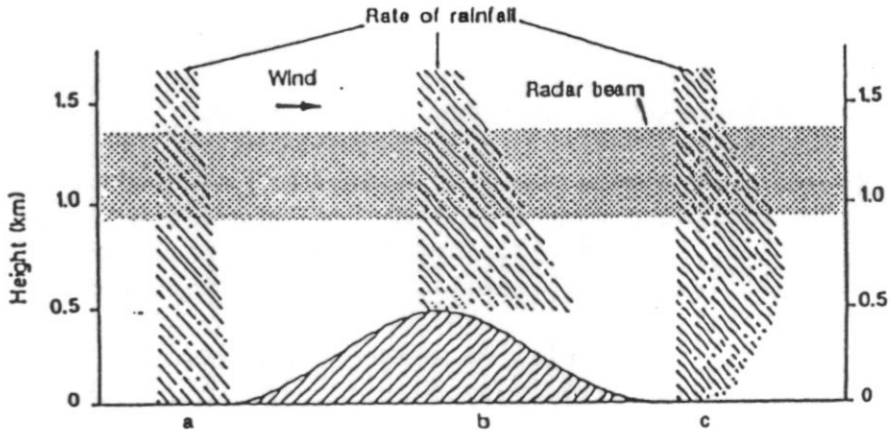

Figure 2.2 Orographic enhancement; assumed rainfall/altitude profiles (a) upwind of (b) on (c) downwind of hill

background value at sea level, and the orographically enhanced rainfall is assumed to be proportional to P_o and the height, h, of the high ground, such that

$$P_o = \alpha h P_o \qquad (2.1)$$

then by simple algebra the radar Assessment Factor for a perfectly accurate radar can be found for any values of beam height, h, P_o and α.

As shown in Fig. 2.3, the model predicts surprisingly complex behaviour for values typical of the Bowland Fells: AF diminishes with increasing beam height for all assumed values of high ground height h, and does so more rapidly for higher ground; however for higher ground levels and lower beam heights, AF values will exceed upwind values and may even exceed 1, whereas AF values are reduced by orographic enhancement by lower ground and higher beam heights. Though not quantified, it is clear from Fig. 2.2 that very large values of AF may be found because of low-level evaporation in rain shadows.

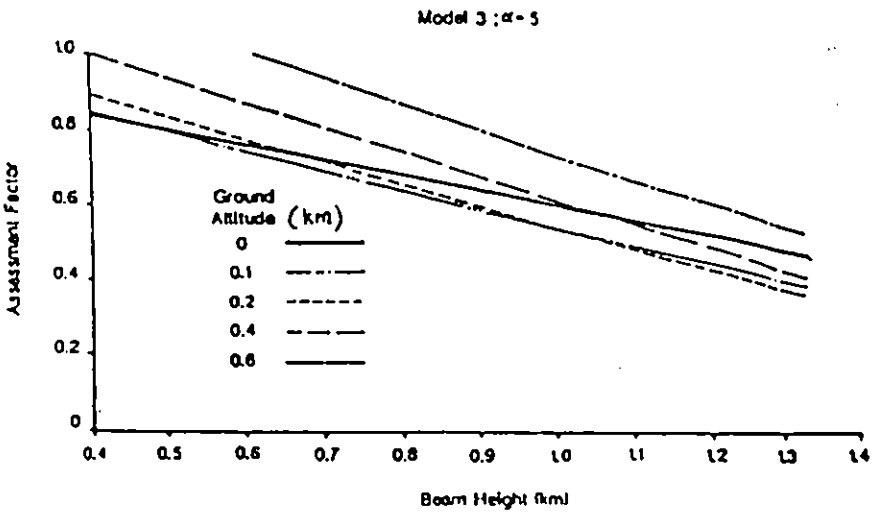

Figure 2.3 Orographic enhancement model: influence of beam height on Assessment Factor

Data from the Bowland Fells study have been used to test the general features of the model. Figure 2.4 shows the distribution of AF with beam elevation in a case of very strong enhancement (rainfall rates rising from less than 1 mm/hr on the plain to over 6 mm/hr on the high ground - corresponding to an α value of 18). Points of correspondence with Fig. 2.3 are i) AF values at high beam heights are reduced over higher ground, and ii) the profile from the upwind plain crosses the profile from the upwind sides of the Fells. Note that very large AF values are observed in the lee of the Fells.

On other occasions, the observed behaviour was much more complex. Southerly winds show smaller orographic enhancement, possibly because the irregular upwind topography there disrupts the flow of the moist feeder flow. In fact an exhaustive study of radar and gauge observations of orographic enhancement in the Bowland Fells (Brown, to be published) confirms that the degree and distribution of orographic enhancement varies strongly with the orientation, speed and meteorological condition of the impinging air streams, and can vary rapidly in time and space during any

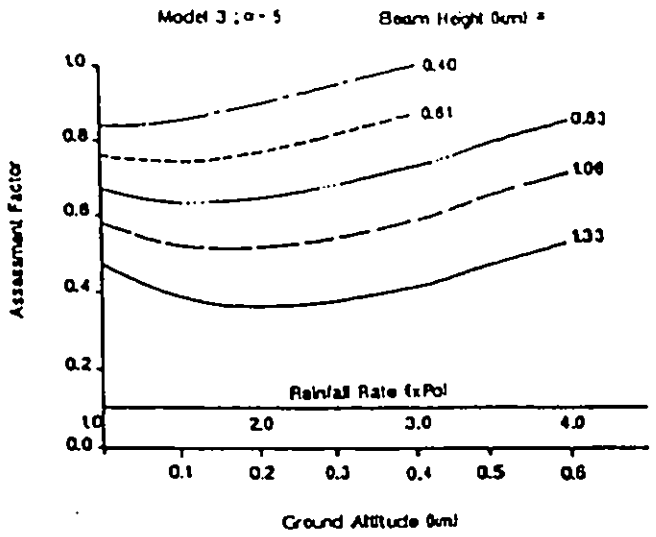

Figure 2.4 Orographic enhancement model: influence of ground altitude on Assessment Factor

particular event. In particular, great care is needed in defining the background precipitation level on the upwind side of the hills (especially if this lies in the rainshadow of adjacent high ground), and in selecting the best measure of the orographic enhancement.

2.3.2 Range studies

Initial studies on the small Bowland Fells area showed that in widespread rain, AF values decreased with increasing range from the radar for over 80% of the time (Collinge 1989,) confirming the evidence of Collier(1986). Following the extensive examination of the relationship between R_g and R_r independently of AF (see 2.4 below), data from 63 hours of widespread rainfall within 75 km of Hameldon Hill were analysed for a relationship with range D in the form

$$R_g = a R_r^b D^c. \qquad (2.2)$$

Mean square errors between R_g and R_r were minimised in 36 hours of data when this relationhip was used, as compared with 12, 11, 5 and 1 hours of data when errors were minimised by respectively replacing D by beam height, ground height, head room (the difference between the previous two) and nothing. It is clear therefore that a significant range relationship exists in these data.

Further studies of the same data showed that the exponent c of range D in the above equation lay between 1.5 and -0.1, with an average of 0.27 and a standard deviation of 0.25. To investigate the origin of the large spread of c values, the data were

reanalysed separately for differing rainfall distributions, some showing significant orographic enhancement.

Heavy rain spreading across the area (i.e within 75 km of the radar) was associated with statistically significant c values between 0.98 and 0.26. Strong orographic enhancement with distinctly heavier rain to the north of Hameldon Hill was significantly associated with smaller c values (0.28 - 0.53), whereas orographic enhancement associated with more uniform north-south rainfall distribution was less significantly associated with even smaller c values.

Application of the above equation to bright-band data shows that introducing range D produces only a small reduction in the mean square error, which contrasts sharply with events having no bright-band effects, presumably because of their smaller range of radar reflectivities. Further details are found in Collinge (1990).

Note that range effects were not investigated in the later study of the full 210 km range from Hameldon Hill, but that the procedure followed there (of applying a fixed correction surface before calibration) would have the effect of implicitly correcting for any consistent range effect in the data.

2.3.3 Blocking effects

Initial studies of the smallest area showed that there were several anomalies in the Hameldon Hill radar images which needed correction before further work could usefully proceed. The first to be noticed were radial shadows caused by a TV transmitter mast close to the radar, occultation by Pendle hill 13 km North of the radar and gross underestimation very close to the radar(radius $<$ 5 km). The first and last of these were not addressed by on-site correction, but the Pendle occultation was. It is therefore clear that routine corrections were inadequate in number and degree, and that some unknown instrumental factor was drastically reducing sensitivity to very close echoes.

To correct for these anomalies it was assumed that over a substantial period of time the aggregated radar-derived rainfall in any pixel should be proportional to the average annual surface rainfall (from maps of average rainfall from 1941 to 1970). Radar data were aggregated for 6 rainfall events totalling 146 hours, and correction factors calculated. For the Pendle anomaly, corrections were calculated on a row-by-row basis, using a pixel just to the east of the anomaly as reference (Fig. 2.5). Even larger corrections (up to x 2.7) were similarly calculated for the TV mast shadow. Subjectively, the corrected radar-derived rainfall patterns were judged to be greatly improved.

When the research area was extended to the 75 km radius, the first two anomalies were seen again, together with further substantial anomalies, again mostly caused by inadequate or incorrect on-site correction for occultation. However, the cause of one zone of overestimation by radar in both the 0.5 and 1.5° beams has not been

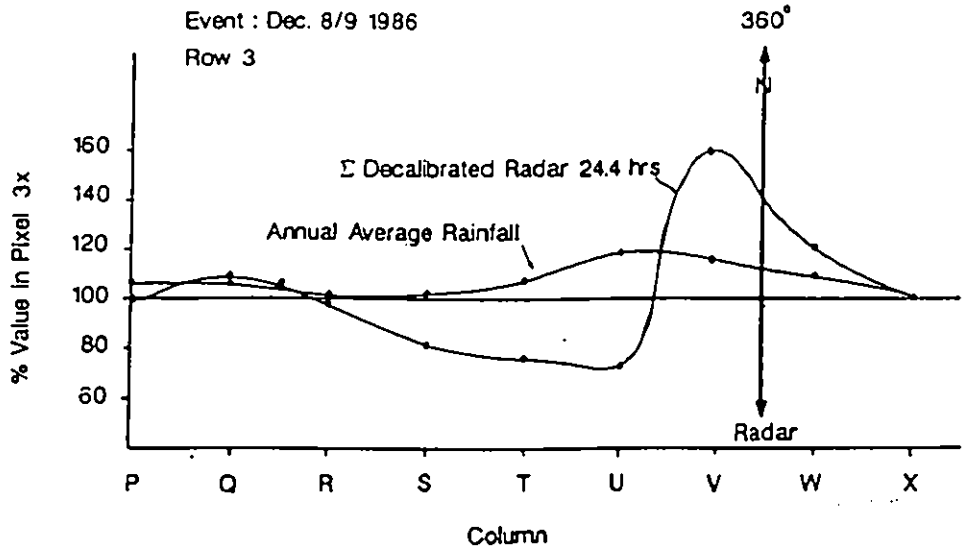

Figure 2.5 East-West section through the Pendle Hill Anomaly at a range of 58 km

identified. Corrections for three of these anomalies (the same three as in the original small area) were applied to subsequent analyses of radar data using a multiplier correction surface fixed in time but variable in space.

When the area of study was extended out to the 200 km radius (pixel size 5x5 km^2 over the whole area), the same anomalies were found to extend to the full reported range, often with greater severity than at shorter ranges (Fig. 2.6). Corrections were determined by comparing interpolated gauge rainfalls for the whole of 1989 with the corresponding radar totals, finding a log correction factor (log R_g/R_r) for each of the 1400 gauges, interpolating to find a log correction factor for each pixel, and antilogging these to correction factors. The resulting radar correction surface for Cumbria was tested on 3 frontal rainfall events by fitting calibration surfaces (time variable surfaces found by spatially interpolating hourly values of CF = 1/AF) with and without the the fixed correction surface using various combinations of gauges as calibrators and controls. In this way substantial reductions were found in discrepancies between calibrated radar rainfalls and gauge rainfalls when the correction surface was included (Archibald, 1991).

It is clear that the pretreatment of fixed anomalies facilitates the subsequent application of variable correction factors. The success of the procedure with the long range data, strongly suggests that it would have been better to correct the 2 km pixel radar data using a full year's radar data (rather than only 146 hours), had the data costs not been prohibitive. It is also clear that the elegant and objective method of assessing the effectiveness of the fixed corrections to the 5 km pixel data should be applied to all such corrections in future.

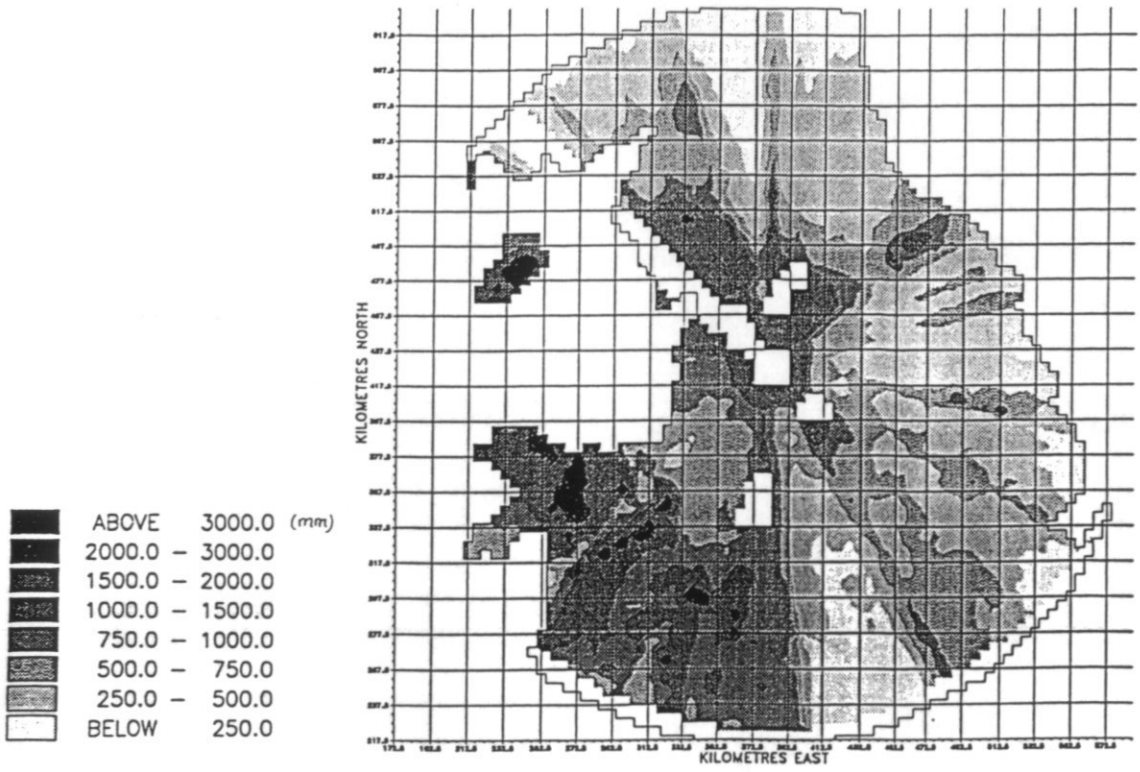

Figure 2.6 Annual rainfall total recorded by the Hameldon Hill radar in 1989

2.3.4 Convection

Although early studies of shower clouds by radar usefully outlined the shapes of their cores of precipitation, it has long been recognized that quantitative measurement of showery precipitation by radar is fraught with problems, and that calibration against ground truth is rarely feasible, given the wide spacing of telemetering gauges in comparison with the narrow precipitation cores (Zawadski, 1984). The occurrence of a severe and damaging convective storm (the Halifax Storm - Collinge et al., 1989) within a few tens of kilometres of the Hameldon Hill radar on 19 May 1989, allowed close scrutiny with good radar coverage and comparison with gauge readings.

Radiosonde data from Aughton, 50 km to the WSW, show strong convective instability throughout the troposphere at the time of the storm's outbreak (1200 GMT), fed by a pool of warm moist air lying over central northern England. The 2km radar imagery from Hameldon Hill revealed complex development of small transient cells of intense echo which collectively persisted for over 6 hours (Fig. 2.7). Comparison with storm totals of at least 5 mm from 22 gauges in the area, increased by 9 by including 15 minute totals from the two recording gauges (scaled up to equivalent storm totals), gave 31 values to fit into the expression

$$R_g = a R_r^b \qquad (2.3)$$

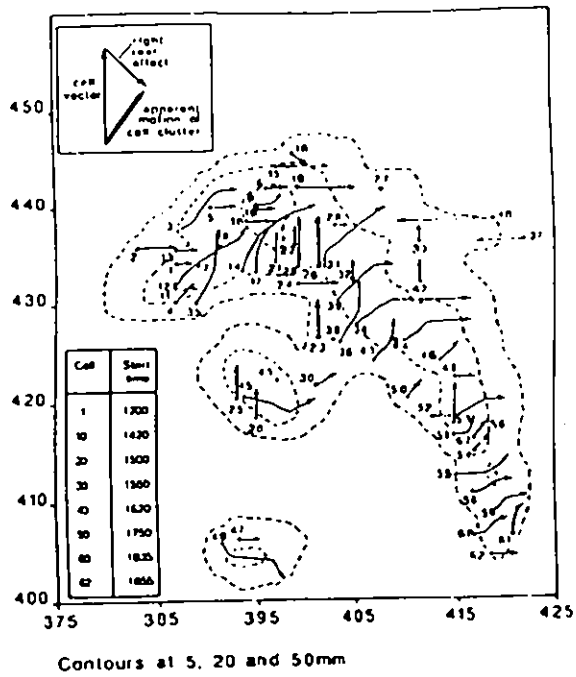

Figure 2.7 Movement of individual storm cells (insert - cell cluster movement in relation to movement of individual cells)

with the result shown in the dashed line in Fig. 2.8. The exponent b has value 0.90 and standard error 0.25, and the factor a has value 1.14, which means that the relationship is probably not significantly different from $R_g = R_r$. Note that the b value is about double that found in non-showery precipiation (Section 2.4.).

Storm average Assessment Factors at the gauge locations were distributed roughly normally from 0.2 and 0.26 for the two gauges recording most rain (193.2 and 80.0 mm respectively - though the former has not been accepted as reliable by the Meteorological Office), to 2.8 for a gauge reading 10.8 mm. The mean of log AF was equivalent to an AF value of 1.2. Several gauges not included in the above data set read zero, though the radar observed significant rainfall overhead (giving infinite AF). A strong tendency of radar to underestimate high convective rainfall rates is apparent in these values and Fig. 2.8. The relatively large area of the pixels (4 km^2) in comparison with the likely areas of intense precipitation cores must smooth the peak values which would be observed in higher resolution radar images. The relatively open gauge network will miss many of these cores, but small AF values will result where they do not. It would therefore seem to be unsafe to use radar underestimation to discount an extreme gauge value as was done by the Meteorlogical Office for this storm.

Further analysis of the 31 values, adding radar range, D, or beam height, H, to the R_g:R_r relation suggested a probably significant variation as H^2, which implies AF variation as H^{-2}.

The complex structure of the radar images comprising Fig. 2.7, has been reanalysed using objective contouring, for further analysis of cell initiation, movement and decay. Computer animation of the sequence suggests possible influence by topography and surface type. Further study of the very low AF values associated

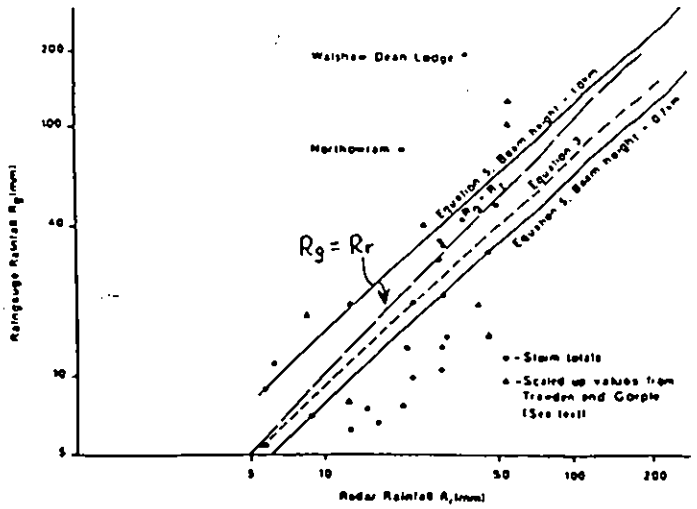

Figure 2.8 Relationship between raingauge rainfall and radar rainfall

with the greatest gauge rainfalls indicate the likely nearby presence of very strong gradients of echo, with consequent underestimation by averaging across the relatively large pixels. Comparison of radar data from the four beam heights is unfortunately not very revealing because the storm remained very close to Hameldon Hill throughout its active life. Despite the obvious difficulties, it seems likely that properly interpreted radar data have considerable potential for the assessment of convective rainfall.

2.4 CALIBRATION AND ASSESSMENT

2.4.1 Introduction

Work on the Hameldon Hill Case Study concerning calibration has focussed on looking for relationships between the decalibrated (section 2.2) radar rainfalls R_r and gauge rainfalls R_g, each totalled over periods ranging from 15 minutes to a year. The radar rainfall data from Hameldon Hill implicitly assume a relationship between radar reflectivity and rainfall rate of the form

$$Z = 200\ R_r^{1.6} \qquad (2.4)$$

(with 200 operationally replaced by 300 in conditions judged to be showery). Since there was no realistic way of replacing this with the several different relationships suggested by Austin's (1987) work in varying meteorological conditions, the resulting Rr values from Hameldon Hill were simply accepted for subsequent close comparison

with raingauge data.

After correction for obvious blocking effects (Section 2.3), corrected R_r values were compared with gauge data by a variety of statistical methods, which are described in the following two sub-sections called Bulk Analysis and Time Series Analysis.

2.4.2 Bulk Analysis

Initially radar Assessment Factors were derived for hourly totals at calibrating gauges. However the appearance of an apparent connection between AF and rainfall rate (R_r or R_g) highlighted the statistically unsound practice of using AF, a parameter defined by a ratio of rainfall rates. It was therefore decided to examine the relationship between R_g and R_r in the form

$$R_g = f(R_r) \tag{2.5}$$

and look for the most successful form of the function f.

Out of four different forms of the function f which were tested, the most successful was found to be

$$R_g = a R_r^b \ , \tag{2.6}$$

success being judged by the criterion of minimum mean square error (between 'predicted' and actual R_g), using an optimising algorithm specially devised for the work.

Once this functional relation was established, the more conventional regression using the logarithm of the equation was used because of its greater speed and stability. Its drawback of giving too great weight to small rainfall values was reduced by discarding all values of R_r and R_g less than 0.2 mm. Applied to 63 hours of non bright-band data from the 75 km range from Hameldon Hill, values of a and b in the above equation were found to be

	a	b
Average	1.96	0.64
Standard deviation	0.56	0.25

The values for b strongly suggest a nonlinear relationship between R_g and R_r, whose simplest interpretation is that the operationally assumed Z/R_r relation was not the most appropriate for these conditions.

To investigate physical explanations for this behaviour, values of a and b were

calculated over the 75 km range for successive hours in several frontal rainfall events. Figure 2.9) is fairly typical, showing consistent, apparently coherent variations in the exponent b, and larger, less coherent variations in the coefficient a. Minimum values of a often seem to occur during the passage of the frontal rain, which may simply indicate weakening relationship between R_g and R_r in the disturbed conditions. Much higher values of the exponent b (approximately 1) were found in 7 hours of data, mostly as rather light frontal rain was becoming established over the area.

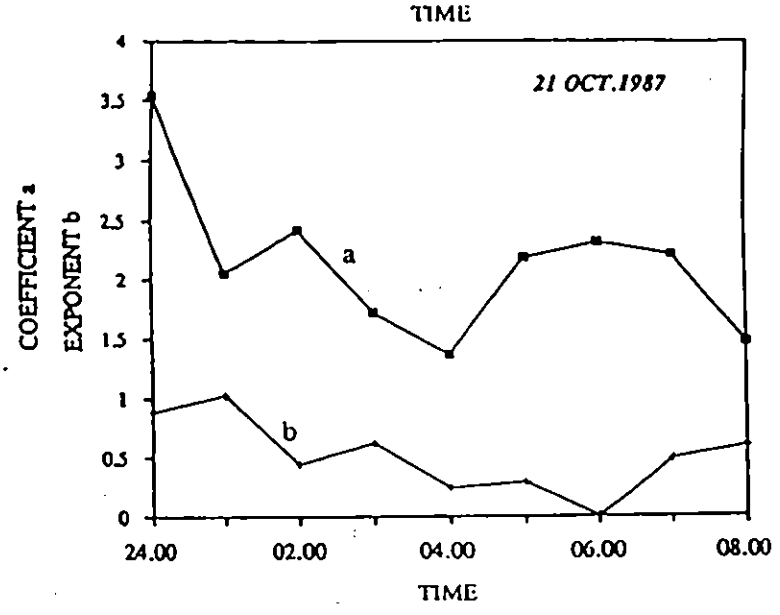

Figure 2.9 Changes with time of coefficient a and exponent b

Another way of investigating variations in a and b, was to look for statistical associations with and between factors describing distributions of R_r and R_g. Out of 11 such measures tried, the two most illuminating results are shown in Figs. 2.10 and 2.11. The former shows, as already expected, that the exponent b reduces with the correlation between R_g and R_r. The latter shows how the exponent b tends toward a narrow range of values centred on about 0.5 as the average gauge rainfall (over the whole 75 km range) increases above about 2 mm. This is particularly obvious when 7 data points with low R_g:R_r correlations and low b values (associated with the passage of fronts) are ignored

This analysis was extended by adding in turn a term in range D, beam height, ground height and head room, with results outlined in Section 2.3.2.

As noted in 2.3.3 above, substantial improvements in calibration of the 200 km range, 5 km pixel radar data were noted when a good anomaly correction surface was included. Very importantly, the improvement was not limited to the anomalous zones

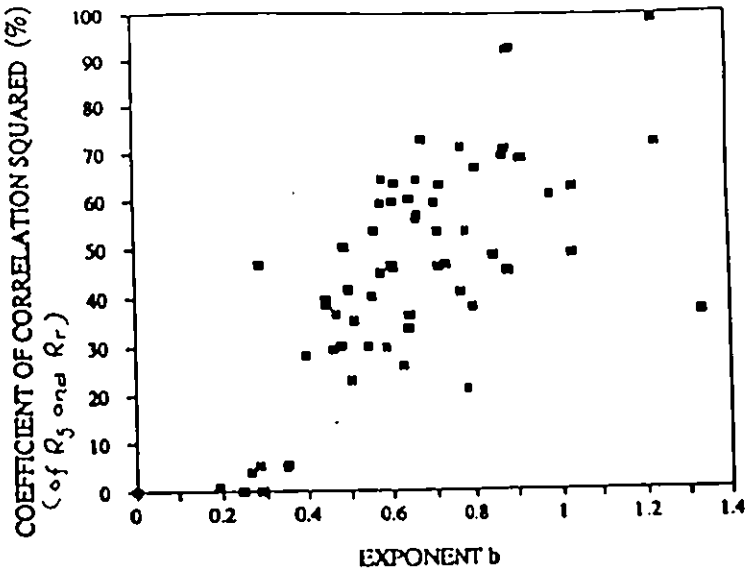

Figure 2.10 Relationship between the exponent b and the resulting coefficient of correlation squared

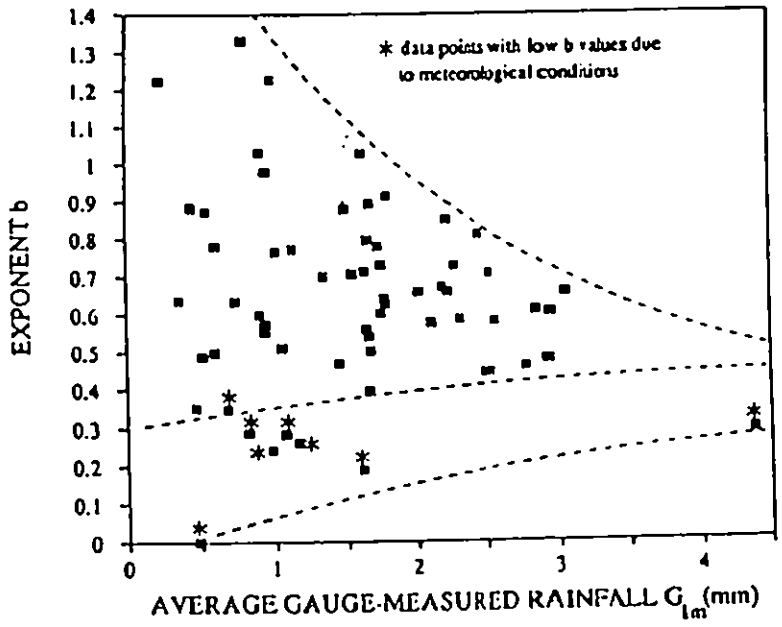

Figure 2.11 Influence of average gauge-measured rainfall G_{lm} on exponent b.

for which the correction surface was principally devised. It was further found that calibration gauges could be chosen much more freely over the whole area when the correction surface was included (rather than be sited in and just outside the anomalies), and that their number could be reduced (from 12 to 4) by the elimination of the less effective gauges. Full details of this phase of the work will be available in Archibald (1991).

2.4.3 Time series analysis

The conventional operational calibration procedure (and indeed the above special analyses) treat successive instantaneous or averaged measurements as independent, though coherence in time is clearly observed (e.g. Fig. 2.9). To include the important constraint of temporal consistency, time series analysis techniques were applied to the linked series of gauge and radar measurements $(R_g)_k$, $(R_r)_k$, where k indicates that these measurements were made in the kth time interval. The regression was found to work best in the form

$$(R_g)_k = CF_k(R_r)_k + e_k \qquad (2.7)$$

where e_k is a random sequence with zero mean and variance, σ_e^2 and CF_k is the calibration factor ($1/AF_k$) which varies as a random walk

$$CF_k = CF_{k-1} + \eta_{k-1} . \qquad (2.8)$$

η_{k-1} is a second random sequence with zero mean and variance, σ_η^2. With this formulation, the series CF_k can be found using Kalman Filter techniques (Young 1984) provided the noise variance ratio (NVR = σ_η^2/σ_e^2) is defined; NVR was taken to be 0.01.

The method was applied to a number of different widespread rainfall events affecting the 60x80 km^2 study area, and analysis confirmed that the error sequences were indeed random. CF_k's were calculated for the calibrating gauges for each 15 minute time interval (k-1), and one-step-ahead (k) values calculated from the above. These values were then applied to predict one-step ahead rainfalls $(R_g)_k$ at neighbouring test gauges, and the results compared with those produced by the conventional method. Mean square errors showed that the new method was usually somewhat better than the old, and that the improvement was sensitive to the choice of calibration gauges. The improvement increased further when log CF_k was regressed against radar range D to allow for the expected attenuation with increasing range (Section 2.3.2). This promising combination of time series and spatial analysis is reported in Collinge (1989 a and b) and forms a continuing topic of research. The ability of the method to match R_r and R_g at a site is dramatically shown in Fig. 2.12.

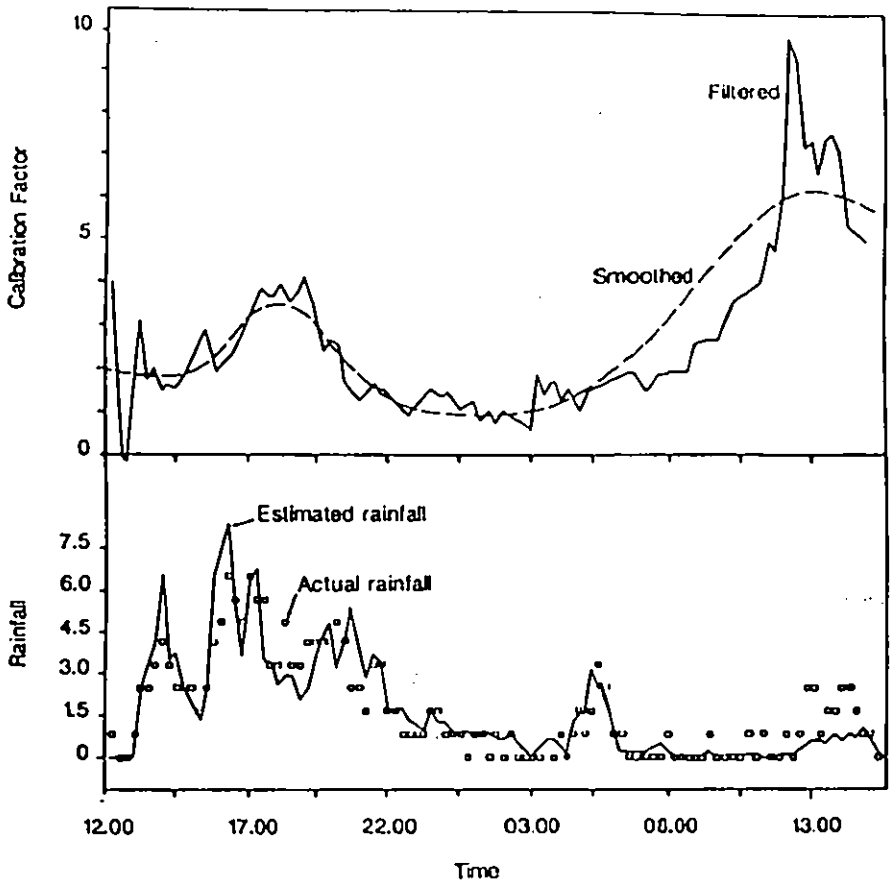

Figure 2.12 Application of Time Series Method 2 to one rain gauge site, 3rd/4th December 1986. Filtered and smoothed estimates of CF (above) and estimated and actual 15 minute rainfall values (below)

3. Local Calibration of Weather Radar: The London Case Study

3.1 INTRODUCTION

A once-in-50 year flood in the London area can cause damage to residential properties approaching £17 m (Haggett, 1986). Substantial potential savings exist if timely and accurate warning of imminent flooding can be given. The London Weather Radar Local Calibration Study was initiated in recognition that weather radar data from the Chenies radar serving the London area can contribute to the realisation of these potential savings. Chenies weather radar provides a unique source of information on rainfall variations over London and its surrounding area.

The main aim of the Study was to use the 30 telemetering raingauges available for the London and Lee Valley area (Figure 3.1) as the basis of a regional calibration procedure. An existing calibration performed at the radar site used only 5 raingauges as part of a domain-based calibration procedure (Collier et al, 1983): this introduced

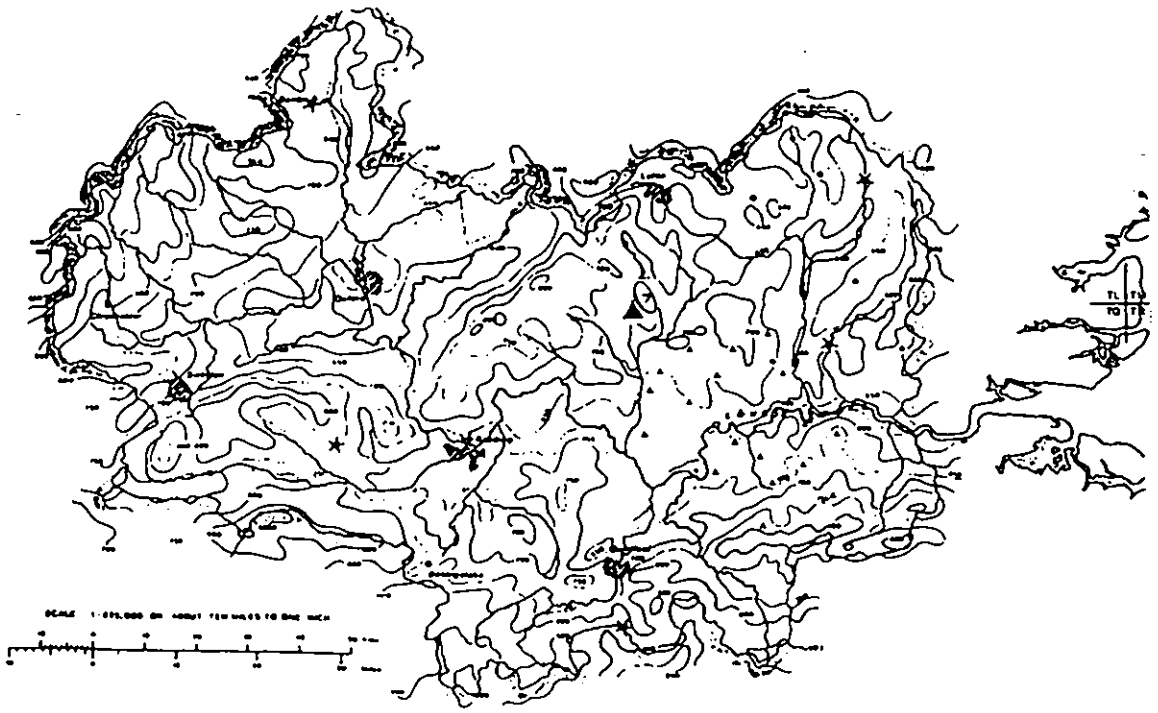

*Figure 3.1 Locations of the radar and raingauges within the Thames basin and annual average rainfall in mm (Δ London raingauges; • Lee Valley raingauges; * Meteorological Office "at-site calibration" gauges)*

discontinuities in the radar field at the domain boundaries. The aim was to produce a smooth adjustment procedure employing the full raingauge network, providing more accurate and reliable estimates of spatial rainfall variations, in particular to support flood warning operations. The main focus of the Study was the development of procedures for the calibration of weather radar based on fitting surfaces to the calibration factor values, conventionally defined as the ratio of raingauge to coincident weather radar grid-square estimates of rainfall. Consideration was given to a wide range of calibration procedures. A comprehensive program for the assessment of the different calibration methods was developed as the major data-analytic tool for the Study. Some important aspects of the Study are highlighted in this paper together with an outline of the procedure finally adopted for operational implementation. Further details are provided in (Moore et al, 1989a, 1989b and 1991).

3.2 THE SURFACE FITTING METHOD

A range of options for combining radar and raingauge data are considered in Moore (1990). These range from space-time models of the rainfall field, which incorporate the covariance structure of the rainfall field and measurement errors, to simpler formulations based on optimal linear interpolation (Gandin, 1965; Jones *et al.*, 1979), Kriging (Matheron, 1971; Creutin and Obled, 1982) or surface fitting. It is the last technique that has been adopted, for reasons of computational efficiency, directness of approach and simplicity. In fact strong links between surface fitting, optimal interpolation and Kriging can be established (Lancaster & Šalkauskas, 1986). Whilst the latter two techniques decompose the problem into constituents which require specification of the spatial correlogram or variogram, the surface fitting provides a simple and direct method of merging radar and radar data in which uncertainties are accomodated implicitly through the method used to fit the calibration factor surface. The basis of the method is to fit a mathematical surface to calibration factor values calculated at n raingauge locations and to scale the radar rainfall field by the coincident factor values to derive a more accurate calibrated radar field. As a result of trials, the specific definition of calibration factor adopted was $z_i = (R^i_g + \epsilon_g)/(R^i_r + \epsilon_r)$. Here R^i_g and R^i_r are the i'th raingauge measurement and the coincident radar grid-square value for a 15 minute interval. The parameters ϵ_g and ϵ_r are small constant values which ensure that the calibration factor is defined for radar values equal to zero.

The particular surface fitting method adopted is based on an extended form of the multiquadric presented by Hardy (1971). First, let z_i be the calibration factor values defined at the n raingauge locations, having grid coordinates $\underline{x}_i = (u_i, v_i)$. The multiquadric calibration surface is defined as the weighted sum of n distance, or basis functions centred on each gauge; that is

$$s(\underline{x}) = \sum_{j=1}^{n} a_j \, g(\underline{x}-\underline{x}_j) + a_0 \qquad (3.1)$$

where $\{a_j, j=0,1,2,\ldots,n)$ are parameters of the surface. The distance function adopted as a result of trials was the simple Euclidean distance

$$g(\underline{x}) = \|\underline{x}\| = \sqrt{(u^2+v^2)} \tag{3.2}$$

which corresponds to building up the surface from a set of n right-sided cones, each centred on one of the n raingauge locations.

Formally, estimation of the a_j weights is achieved as follows. Equation (1) for

$$s(\underline{x}_i) = \sum_{j=1}^{n} a_j\, g(\underline{x}_i - \underline{x}_j) + a_0 = z_i \qquad (i=1,2,\ldots,n) \tag{3.3}$$

may be expressed in matrix form as

$$\underline{G}\,\underline{a} + a_0\underline{1} = \underline{z} \tag{3.4}$$

where $\underline{G}$ is an n by n matrix with the (i,j)'th element given by $G_{ij} = g(\underline{x}_i - \underline{x}_j)$, $\underline{1}$ is a unit vector of order n, and $\underline{z}$ is the vector containing the n calibration factor values. As one approach to avoiding anomalies in the surface form away from n raingauge locations, an additional requirement for flatness at large distances is imposed through the constraint

$$\underline{a}^T\underline{1} = 0. \tag{3.5}$$

For the Euclidean distance function of cone type this constraint corresponds to a requirement of zero-slope with increasing distance from the raingauge network. Solution of equation (4) subject to constraint (5) for the weighting coefficients gives

$$\begin{aligned} a_0 &= (\underline{1}^T\underline{G}^{-1}\underline{z})/(\underline{1}^T\underline{G}^{-1}\underline{1}) \\ \underline{a} &= \underline{G}^{-1}(\underline{z} - a_0\underline{1}) \end{aligned} \tag{3.6}$$

It was found to be important to form a conservative calibration factor surface by adopting a fitting method which allowed the surface to depart from the actual calibration factor values. This was achieved by allowing the Euclidean distance $g(\underline{x}_i - \underline{x}_i) = g(\underline{0})$, normally zero, to take a value -K. This results in a surface which passes within a distance a_i K of the calibration factor value for the i'th raingauge. The problem of discontinuities is avoided by using this form in the estimation of the weights, a_j, and using the normal form in calculating the surface values for radar calibration of the full field. The constraint of equation (5) ensures that the "errors", introduced by using $g(\underline{0}) = 0$ in equation (1) (and not -K) when forming the surface for calibration, add up to zero.

An illustration of the form of a fitted surface and the resulting calibrated radar field are shown in Figures 3.2 and 3.3.

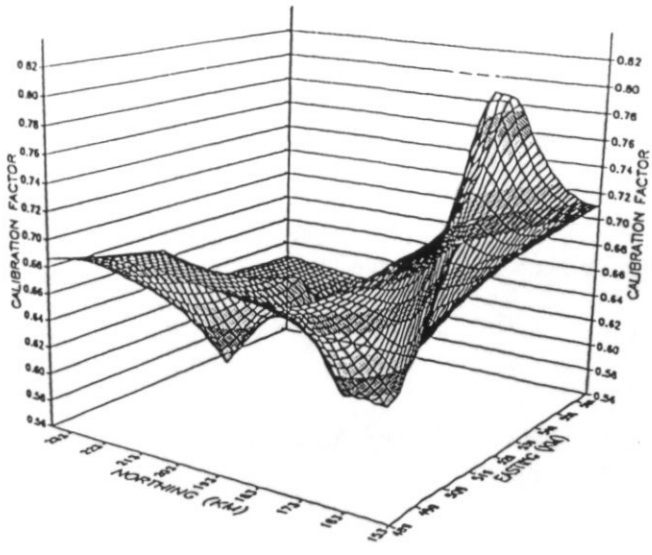

Figure 3.2 Calibration factor surface for 16.30 14 March 1989

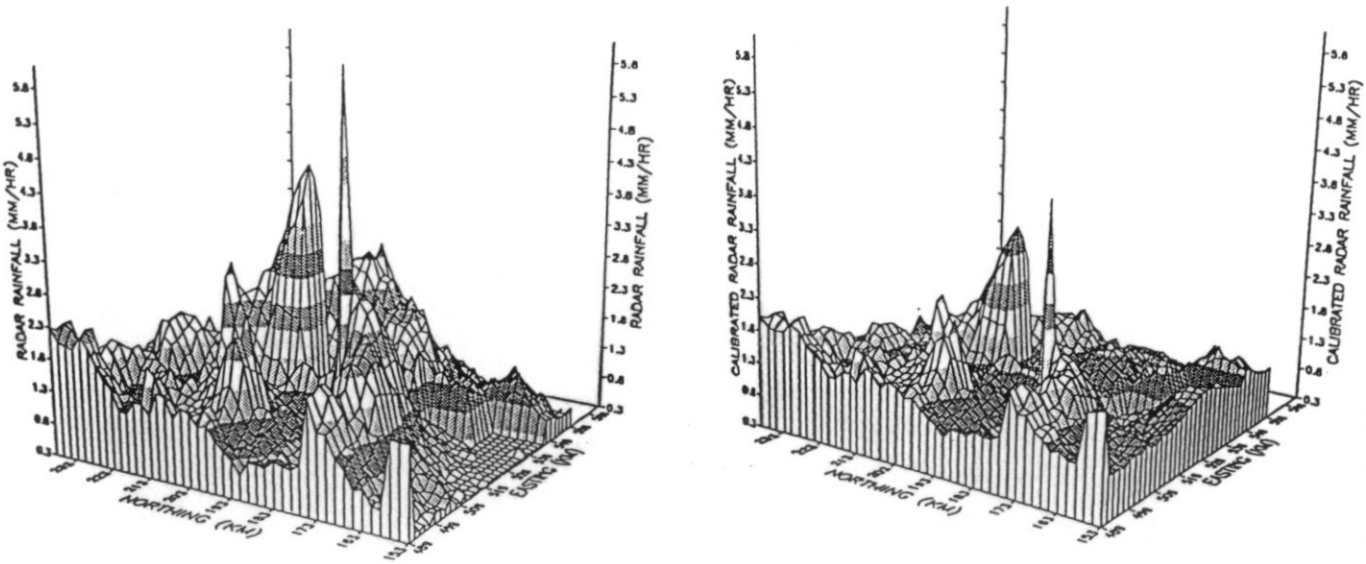

Figure 3.3 Radar fields for 16.30 14 March 1989 before and after calibration

3.3 ASSESSMENT OF METHODS

The Study considered many variants of the above procedure before recommending it for operational implementation. Seven forms of calibration factor definition were evaluated, including reciprocal, trimmed and logarithmic formulations. Account was taken of the position of a gauge within the radar grid square by forming calibration factors which used the average of nine, four or one grid-squares as the radar value.

The choice of a coarser time-interval than 15 minutes for constructing the calibration factor surfaces was also investigated. Compensation for quantisation errors in the raingauge data, due to the use of tipping-buckets, was investigated by forming a conservative calibration factor by incrementing the raingauge value by the bucket increment towards the radar value when appropriate. Different forms of surface, employing smoothed Euclidean, exponential and reciprocal distance functions, were evaluated along with different estimation schemes which minimised surface roughness or constrained the surface to a constant value at large distances.

The assessment was carried out using data from 23 rainfall events over an area of about 60 km by 60 km containing up to 30 raingauges, equivalent to a gauge density of one gauge per 120 km^2 area. A selective deletion procedure was used whereby one gauge was omitted, the surface fitting scheme applied and used to form an estimate of the rainfall at the deleted gauge. This was repeated n times for each gauge giving n sets of rainfall estimation error: repetition of this for all 15 minute rainfall fields making up the 23 rainfall events allowed a pooled log root mean square error performance statistic to be formed. Each variant described above was explored using this strategy and a recommendation for operational implementation was finalised. The space- and time-averaged forms of calibration factor and quantisation correction were not found to be worthwhile implementing on the basis of this assessment procedure.

3.4 ASSESSMENT AGAINST SIMPLE RAINFALL ESTIMATORS

It was judged important to assess the final calibration procedure against some alternative simple rainfall estimation schemes. These included an estimate of the rainfall field using (i) a simple arithmetic average of the available raingauges, (ii) a multiquadric surface fitted to the raingauge values, and (iii) a simple arithmetic average of the calibration factor values. The results are summarised in Table 3.1.

Table 3.1 Assessment of Alternative Rainfall Estimation Techniques

Method	log rmse	% improvement in log rmse
Uncalibrated Radar	.068	0
Raingauge Average	.084	- 24
Surface fitting to Raingauges	.072	- 6
Calibration factor average	.058	15
Surface fitting to calibration factors	.053	22

These show that the radar, without raingauge calibration, is better than an estimate using the raingauge network alone, despite its density and the use of a sophisticated surface fitting interpolation method. Even the application of a simple raingauge calibration applied to the radar data improves the accuracy by 15% and the use of the more sophisticated surface fitting method increases this further to 22%, on average.

3.5 EVENT ASSESSMENT

It is of interest to investigate whether the average increase in accuracy of 22% is achieved uniformly across all events or whether synoptic conditions exert an influence. Table 3.2 provides a breakdown of the performance on an event basis for the uncalibrated radar and the recommended calibration method. Also highlighted are those events which experienced thunder and hence can be generally associated with convective activity. Despite thunder being recorded in 13 of the 23 events only in 3 of these does the calibration procedure cause the rainfall estimate to worsen, and then by only a very small amount. It may therefore be concluded that the conservative nature of the calibration method ensures that rainfall estimation is reasonably resilient to the localised and steep rainfall gradients that make calibration difficult in convective situations. In conditions of widespread frontal rain these results indicate that calibration can improve the accuracy by as much as 45%.

3.6 CONCLUSION

An assessment using data from 23 rainfall events has allowed operational implemementation of the radar calibration to proceed with scientific justification: the Radar Calibration System has now been running successfully since 14 March 1989 in support of flood warning activities over London and the Lee Valley. The assessment indicates that the calibration provides a 22% improvement in accuracy relative to that obtained by the radar without calibration; improvements as great as 45% may be achieved in widespread rainfall and the risk of reducing the average accuracy during localised covective events appears slight. Even without raingauge calibration the radar has been shown to provide better estimates of spatial rainfall than can be obtained using the dense network of raingauges in isolation. An additional procedure which estimates spatial rainfall using only raingauges was implemented in September 1989 to complement the calibration procedure and to replace it in the event that the radar malfunctions.

Table 3.2 ***Assessment of surface fitting calibration method relative to uncalibrated radar on an event basis using the log rmse criterion; T indicates that thunderstorm activity is present for the event***

Event	Uncalibrated radar	Surface fitting calibration method	% improvement in log rmse	
1. Oct 1987a	0.053	0.036	32	
2. Oct 1987b	0.148	0.088	41	
3. Nov 1987b	0.089	0.068	24	
4. Mar 1988a	0.036	0.030	17	T
5. Mar 1988b	0.031	0.022	29	
6. Mar 1988c	0.018	0.012	33	
7. Apr 1988a	0.051	0.048	6	T
8. May 1988	0.064	0.066	-3	T
9. Jun 1988a	0.038	0.032	16	T
10. Jun 1988b	0.115	0.118	-3	T
11. Jul 1988a	0.030	0.029	3	T
12. Jul 1988b	0.044	0.036	18	T
13. Jul 1988c	0.042	0.040	5	T
14. Jul 1988d	0.064	0.066	-3	T
15. Jul 1988e	0.051	0.035	31	
16. Jul 1988f	0.108	0.086	20	T
17. Jul 1988g	0.091	0.056	38	
18. Aug 1988a	0.128	0.117	9	T
19. Aug 1988b	0.063	0.042	33	
20. Feb 1989b	0.081	0.061	25	T
21. Mar 1989a	0.041	0.023	44	
22. Mar 1989b	0.095	0.052	45	
23. May 1989a	0.093	0.056	40	T
Average across events	0.068	0.053	22	

4. Local Rainfall forecasting using Weather Radar: The London Case Study

4.1 INTRODUCTION

The benefits accruing from a radar-based rainfall forecasting system have been assessed at £3.72 m per annum over England and Wales (Collinge, 1989). This assessment was made in the context of the UK Meteorological Office's Frontiers forecasting system (Conway & Browning, 1988) which aims to provide forecasts, updated every half hour, up to 6 hours ahead for a 5 km grid with national coverage. The London Weather Radar Rainfall Forecasting Study was motivated by recognising that the national Frontiers product would not meet the water industry's specific requirements for very short term rainfall forecasts with high resolution in space and time, which are needed particularly for forecasting flooding in urban and smaller rural catchments. Specifically the Study aimed to develop a radar-based rainfall forecasting system with emphasis on forecasting up to two hours ahead every 15 minutes for a 2 km grid extending over an area within a radius of 75 km of the radar. A further requirement was that the system be implemented operationally as part of a regional flood warning system run by the National Rivers Authority Thames Region at Waltham Cross.

The main approach to rainfall forecasting investigated within the Study is one that assumes an underlying advection model and uses simple linear extrapolation to forecast future rainfall fields. This paper presents an outline of the development and assessment of different advection-based radar rainfall forecasting methods which provided the foundation for recommending the forecasting system now in operational use over London and the Thames basin.

4.2 RADAR RAINFALL FORECASTING METHODS

An advection model of rainfall field movement forms the basis of all forecasting methods considered in the Study (Moore et al, 1991). Simple linear extrapolation is used to project the current radar rainfall forward, according to the advection velocity, to form forecast fields at successive lead times. The velocity vector is inferred from the current and a previous radar rainfall field by identifying a displacement of the latter which best matches the former.

Formally, using x and y to denote location on the west-east and south-north axes respectively, the x-component of the storm velocity, v_x, is derived from the following

description of rain cell position:

$$x(t + \tau) = x(t) + v_x\tau \tag{4.1}$$

where x(t) denotes the position on the x-axis at the forecast time origin t and τ is the lead time of the forecast. Inference of the velocity vector (v_x,v_y) uses, as the citerion of correspondence, the log root mean square error

$$rmse = \left(n^{-1} \sum_{ij} e_{ij}^2\right)^{1/2} \tag{4.2}$$

where the error $e_{i,j}$ is defined as

$$e_{ij} = \log\{(1 + R_{ij})/(1 + \hat{R}_{ij})\} \tag{4.3}$$

and $R_{i,j}$ is the observed radar rainfall for the (i,j)'th pixel and $\hat{R}_{i,j}$ the forecast amount, based on projecting a previous field at the given velocity. For velocities which do not result in displacements which are integer multiples of the radar grid length the formation of $\hat{R}_{i,j}$ involves the use of the following four-point interpolation formula applied to four adjacent radar cell values:

$$\hat{R}_{ij} = (1-p)(1-q)\ R_{k,l} + p(1-q)\ R_{k+1,l} + q(1-p)\ R_{k,l+1} + pqR_{k+1,l+1} \tag{4.4}$$

Expressions for the position (k,l) and the weights p and q, which depend on the velocity vector (v_x,v_y), are given in Moore et al (1991).

Identification of a velocity pair which minimises the rmse criterion involves a shrinking-grid search procedure at each forecast time origin. A coarse but extensive grid of velocity pairs is initially used and this is progressively reduced over three steps to smaller but finer grids centred on the previous step's best velocity pair. In all three steps only velocities which result in displacements which are integer multiples of the grid length are used in order to avoid the computational expense of interpolation. At the fourth and final step a direct interpolation in the error-criterion field is made, based on a four-point interpolation, to arrive at the final velocity pair to be used for that forecast time origin. Using this approach a velocity inference and two hour rainfall forecast construction over a 76 km radius field requires only 12 cpu seconds on a VAX4200 computer.

Each of the forecast algorithms considered in the assessment incorporate the same radar preprocessing scheme. This provides for automatic detection and correction for persistent anomalies and transient clutter. Also included is a procedure to construct a composite field, incorporating radar data available out to a range of 210 km on a 5 km grid, in order to forecast as much of the target 76 km radius field as possible at higher lead times.

4.3 ASSESSMENT OF METHODS

An evaluation of the above basic advection approach to forecasting against a number of alternatives was carried out using radar rainfall fields from 15 storm events. Preliminary results suggested the use of a hybrid formulation in which the advection forecast, $\hat{R}_{i,j}$, is shrunk towards the field average value, $\bar{R}$, with increasing lead time, τ, so as to produce the modified forecast:

$$\tilde{R}_{i,j} = \begin{cases} \bar{R} + a\left(\hat{R}_{i,j} - \bar{R}\right) & \hat{R}_{i,j} > 0 \\ 0 & \hat{R}_{i,j} = 0 \end{cases} \qquad (4.5)$$

where the shrinkage factor $a = f^{\tau}$, and f is a constant. For the lead times up to 2 hours considered in the evaluation, this hybrid formulation performed better than persistence (a no change forecast), a rain/no-rain pattern matching approach to velocity inference and extensions of the advection method to incorporate acceleration and intensification.

The results of the assessment of a selection of different methods are presented in Figure 4.1. Included in Figure 4.1 are the results of the "best advection" method which is the best attainable forecast using the pure advection approach, derived by inferring the velocity using the current and forecast fields; clearly this is not realisable in practice but provides a useful performance benchmark. Note the anomalous increase in rmse beyond 100 minutes merely reflects sampling effects caused by the progressive loss of the forecast field for higher lead times for some methods (a requirement is imposed for all methods to be able to make forecasts for inclusion in the rmse criterion for a given lead time). In general, the pattern of rainfall forecasts obtained using the hybrid formulation are reasonable up to a lead time of one hour (Figure 4.2).

4.4 CONCLUSIONS

The main conclusions arising from the London Weather Radar Rainfall Forecasting Study are summarised below:

(1) A forecasting method based on an underlying simple advection model and shrinking the forecasts towards the field average value with increasing lead time provides the best performance.

(2) More complex methods incorporating an acceleration or intensification component, or using a rainfall threshold to define a rain/no-rain pattern field from which to infer the advection velocity, did not perform as well.

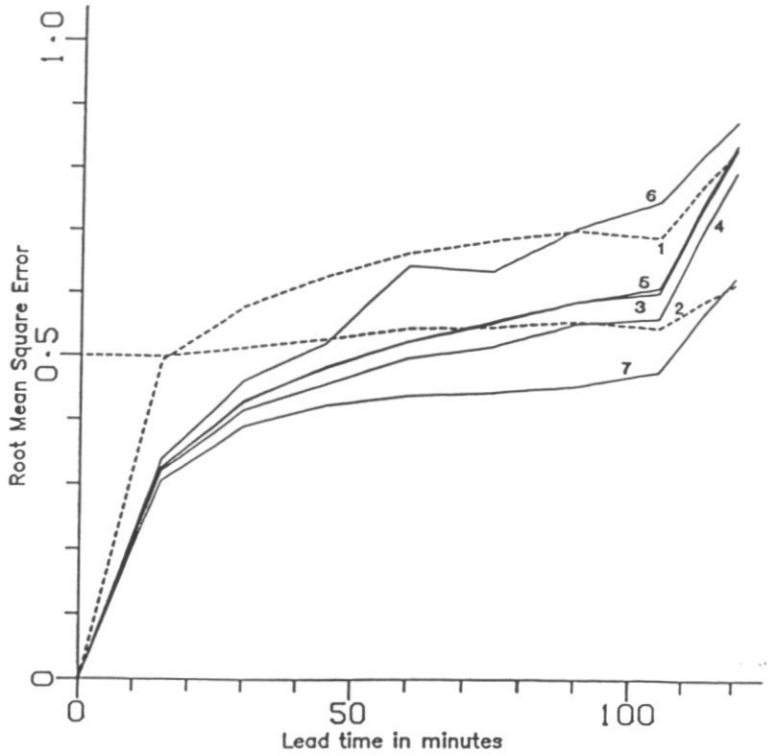

Figure 4.1 ***Assessment of radar rainfall forecasting methods over 15 storm events using the rmse performance criterion. The methods are: 1. Persistence; 2. Field average; 3. Standard advection; 4. Standard advection with shrinkage; 5. Acceleration and advection; 6. Intensification and advection with shrinkage; 7. Best advection.***

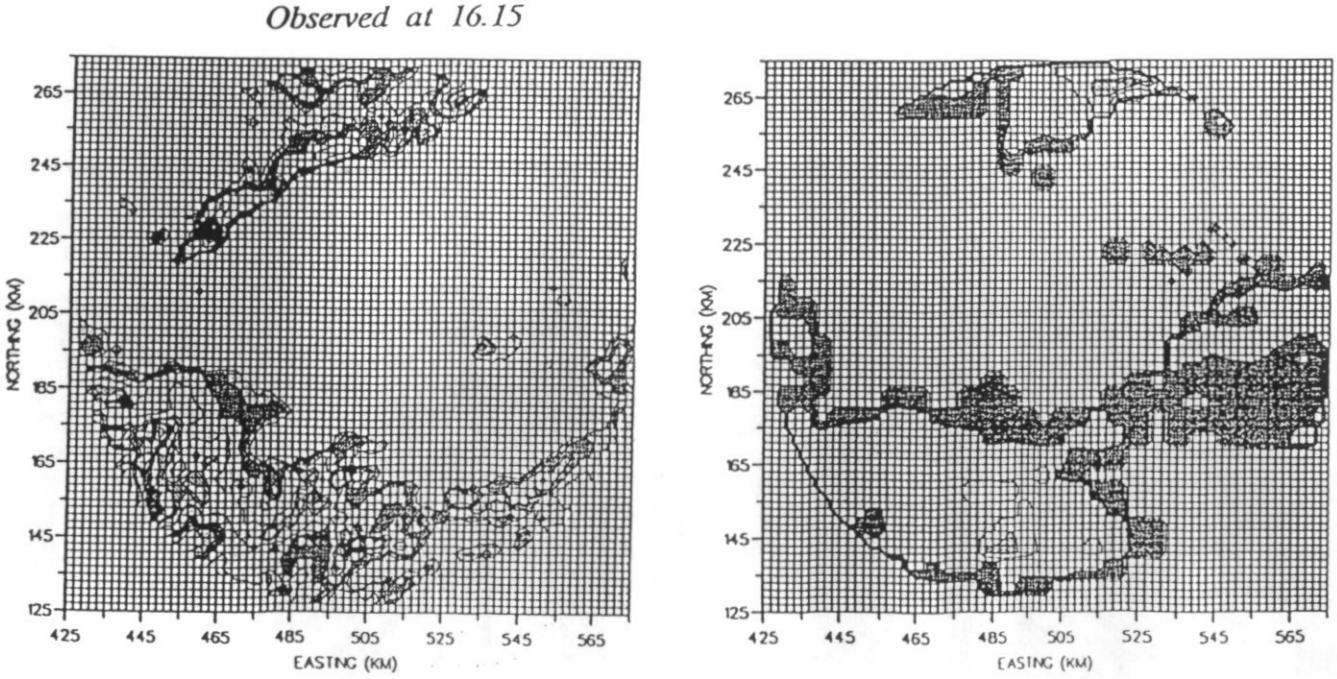

Figure 4.2 ***The observed 76 km radius rainfall field at 16.15 20 December 1989 and the corresponding one-hour ahead forecast made at 15.15***

(3) The general pattern of the forecast rainfall fields are reasonable up to about one hour ahead

(4) A novel shrinking-grid search procedure for identifying the storm velocity from two time-displaced radar images, involving interpolation in the forecast error field in the final step, proved to be both reliable and efficient: a two hour forecast, at 15 minute intervals over a radius of 76 km, is generated in 12 seconds on a VAX4200 using this procedure.

(5) Results obtained have been sufficiently encouraging to proceed with operational implementation.

5. A Grid-square Rainfall-Runoff Model for use with Weather Radar Data

5.1 INTRODUCTION

The traditional approach to modelling the response of a river basin to rainfall is through a lumped representation in which an estimate of catchment average rainfall is used as input. This traditional approach still persists as the most commonly employed approach, particularly for real-time flood forecasting applications. In such applications it is common to require only a forecast at a "basin outlet" location which is gauged and there is little interest in forecasts at internal locations or in a form of model parameterisation capable of predicting the effect of land-use change. Experience has shown that with adequate calibration data in the form of flow records and with only a sparse sampling of the rainfall field using raingauges that more complex, and possibly more realistic, distributed models fail to provide improved forecast accuracy. A common diagnosis is that the models are "input limited" and that improved performance from distributed models will only be achieved when better measurements of rainfall fields are used as input data. Such measurements are now available in the form of weather radar data, commonly available on a 2 km grid at 5 minute intervals.

The aim here is to develop a simple distributed rainfall-runoff model suitable for use in real-time flow forecasting with weather radar providing the source of rainfall input. Whilst it is neither natural nor essential to configure such a model on the radar grid it is the approach which will be investigated here. Such an approach is by no means new: an early example is provided by Anderl et al (1976). The methodology adopted here was first outlined at a symposium in 1987 (Moore, 1991) and preliminary results presented at a workshop in 1990 (Moore, 1992). Other workers have pursued similar lines, but with different model parameterisations, most notably Chander and Fattorelli (1991). Application will be demonstrated using the Wyre basin in north-west England served by a C-band weather radar at Hameldon Hill.

5.2 MODEL FORMULATION

In developing a distributed model suitable for operational use in real-time it is clear that a form of parameterisation is needed that does not involve a large number of parameters in need of optimisation. This dichotomy between the need for distributed parameters and a small number of them needing to be optimised is resolved through the use of contour maps, in the form of digital terrain models (DTMs) if available,

and simple "linkage functions". Contour maps are used in two ways. Firstly, the classical isochrone concept is used to "route" water to the basin outlet, essentially through dictating appropriate time delays as a function of travel paths across hillslope and down river channel pathways. Secondly, the slope of the terrain within a grid-square is used as a control on "runoff production", that is water available for routing rather than absorption by the soil/bedrock. Figure 5.1 provides a simple illustration of these two components which are expanded on below.

The construction of isochrones - lines joining points of equal time of travel to the basin outlet - has been achieved by assuming that water travels with only two velocities depending on whether it is associated with a hillslope or in a river channel. In this way it is relatively easy to construct isochrones by direct inference from the distance of a point to the basin outlet. More complex rules can be introduced, for example including slope influences via a flow resistance equation, given the availability of a DTM. Figure 5.1(b) illustrates a pattern of isochrones superimposed on the radar grid used as the model grid. The areas between isochrones associated with each grid square are calculated and used to apportion runoff from the grid square to a given time delay. In this way a runoff-distributed convolution is achieved to derive the basin flow response at future times.

Formally the convolution of grid-square runoff rate per unit area over a grid square, $r_{t,j}$, from grid squares $j=1,2,\ldots,m$, to obtain the basin runoff rate per unit area over the basin, Q_t, at time t is achieved using

$$Q_t = \sum_{j=1}^{m} \sum_{\tau=1}^{n} u_{\tau,j} \; r_{t-\tau,j} \qquad (5.1)$$

where $u_{\tau,j} = v_\tau \, w_{\tau,j}$. Here, $\{v_\tau, \tau = 1,2,\ldots,n\}$ is the basin unit hydrograph and $\{w_{\tau,j}, \tau = 1,2,\ldots,n; j=1,2,\ldots,m\}$ are the proportions of each isochrone in each radar grid square within the basin. Specifically $w_{\tau,j} = A_{\tau,j}/A_j$ where A_j is the area of the j'th radar grid within the basin and $A_{\tau,j}$ is that part of the area between the τ-1 and τ isochrones. The grid-square runoff rate, $r_{t,j}$, can be chosen to be the direct runoff rate, $q_{t,j}$, or the sum of this and baseflow, that is $r_{t,j} = q_{t,j} + b_{t,j}$. Experience with this simple time-area form of routing subsequently led to the inclusion of an additional nonlinear storage element to represent attenuation effects seen in observed hydrographs. An improved distributed representation of this storage effect is the subject of future work.

Generation of runoff from a given grid-square is accomplished by conceptualising the grid-square as a box-shaped "soil" column. The key element in the conceptualisation is that the depth of the box, and thus the absorption capacity of the soil, is controlled by the average slope within the square as measured from the contour map or DTM. Specifically, the following linkage function is used to relate maximum storage capacity, S_{max}, to the average slope, s, within a grid-square:

$$S_{max} = \frac{(1 - s)}{s^*} \, S^*_{max} \; . \qquad (5.2)$$

(a) River basin with superimposed weather radar grid

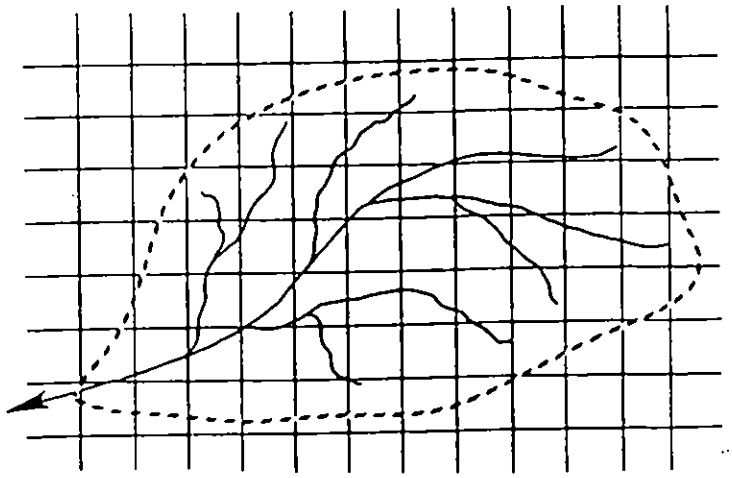

(b) Isochrones for grid-square j

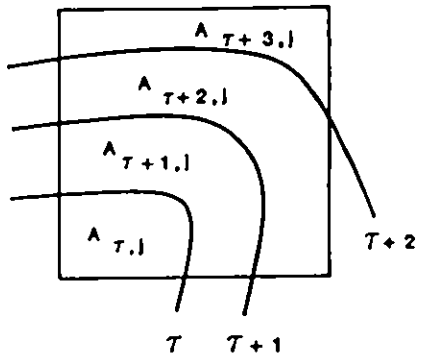

(c) Block representation of runoff response from grid-square j

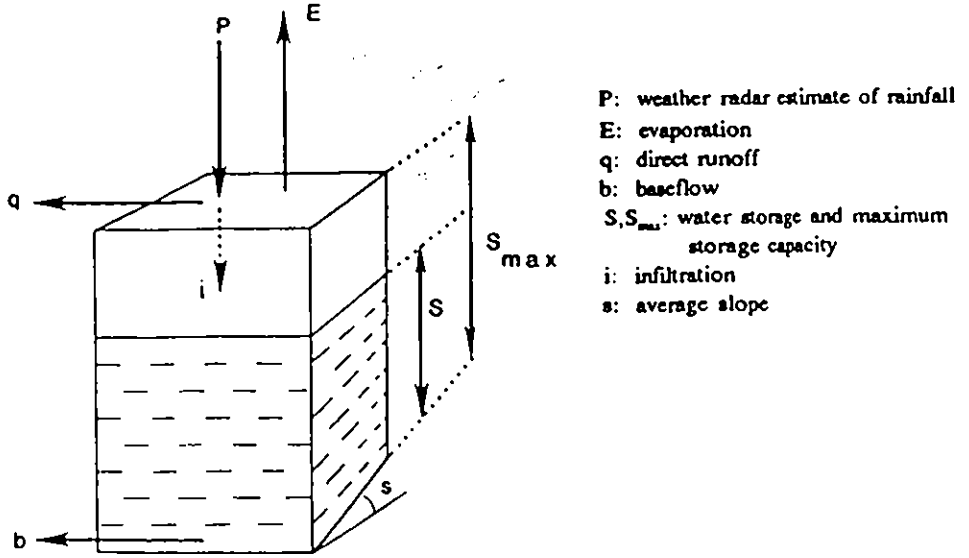

Figure 5.1 Grid-square rainfall-runoff model for flood forecasting using radar data

The parameters s* and S^*_{max} are upper limits of slope and storage capacity respectively and act as "regional parameters" for the basin model. Clearly a measurement of slope for each grid square associated with the river basin can be made from the contour map or DTM whilst parameterisation is achieved for all grids using only these two parameters.

A water balance is maintained for each grid square by using the radar grid-square rainfall as input and introducing soil moisture dependent evaporation and drainage functions. Specifically the balance is maintained as follows for a given box and time interval (ignoring time and space subscripts for notational simplicity). Firstly, a soil moisture dependent infiltration function can be invoked for hydrological environments which experience infiltration-excess, as opposed to saturation-excess, runoff. A potential infiltration rate is given by

$$i_p = \left[1 - \frac{S}{S_{max}}\right]^b i_{max} \tag{5.3}$$

where i_{max} is the upper limit of infiltration rate and S is the water in storage. Then the actual infiltration rate is given by

$$i = \min(p, i_p) \tag{5.4}$$

where p is the rainfall rate. Then direct runoff by this infiltration excess mechanism is simply
q = p - i. (In practice this component is not invoked for modelling the humid temperate basin use in the application that follows).

Drainage from the grid box occurs at the rate

$$b = \begin{cases} \alpha S^{\beta} & S>0 \\ 0 & \text{otherwise} \end{cases} \tag{5.5}$$

where α is a storage constant (units of inverse time) and the exponent β is a parameter (set here to 3). Evaporation loss from the grid box occurs at the rate, E_a, which is related to the potential evaporation rate, E, through the relation

$$E_a = \begin{cases} \left[1 - \frac{D-D^*}{S_{max}-D^*}\right] E & D>D^* \\ E & D \le D^* \end{cases} \tag{5.6}$$

where D = S_{max} - S is the soil moisture deficit and D* is the threshold deficit below which evaporation occurs at the potential rate.

The direct runoff rate is calculated as

$$q = \max(0, S - S_{max}) + p\Delta t - \Delta t. \qquad (5.7)$$

and the updated water storage is given by $\max(0, S + i\Delta t - E_a\Delta t - b\Delta t)$.

5.3 APPLICATION

The above model formulation has been applied to the River Wyre at St Michaels draining an area of 275 km^2 in north-west England. A total of 92 2km square radar grids for the Hameldon Hill radar are associated with its drainage area. Isochrones were constructed assuming translation velocities of 0.1 and 0.5 m/s for hillslope and channel flowpaths respectively. The results presented here concern the forecasting of instantaneous flows at hourly intervals for the month of October 1986 using hourly rainfall totals for the 2 km radar grid and for a raingauge at Abbeystead located within the basin. An assessment of model results using the uncalibrated radar data as a distributed input and then the gauge value as a constant value for the basin revealed problems with the radar measurements of rainfall over this basin. The failure of the radar to always detect rainfall in some areas is known to be attributed to blockage effects caused by a television mast and hills. An attempt to correct for these anomalies was made using the radar anomaly correction method described in Moore *et al.* (1991). Figure 5.2 shows the model forecasts obtained: here the lower dashed line below zero indicates basin soil moisture deficit, the lower continuous line the baseflow, the dashed line the total basin runoff and the upper continuous line the observed basin runoff. These forecasts should be compared with those in Figure 5.3, obtained using only the Abbeystead raingauge value as a spatially uniform input to the grid model. Neither source of data appears entirely satisfactory in sampling the true rainfall field. Further work is planned on basins where radar coverage is less affected by blockage effects.

5.4 CONCLUSIONS

A practical methodology for distributed rainfall-runoff modelling using grid-square radar data has been developed. The problem of over-parameterisation has been circumvented through the use of measurements from a contour map or digital terrain model of the basin together with simple linkage functions. These functions allow many model variables to be prescribed through a small number of regional parameters which can be optimised to obtain a good model fit. Assessment of the model has been frustrated by blockages affecting the radar measurements of rainfall in the study region.

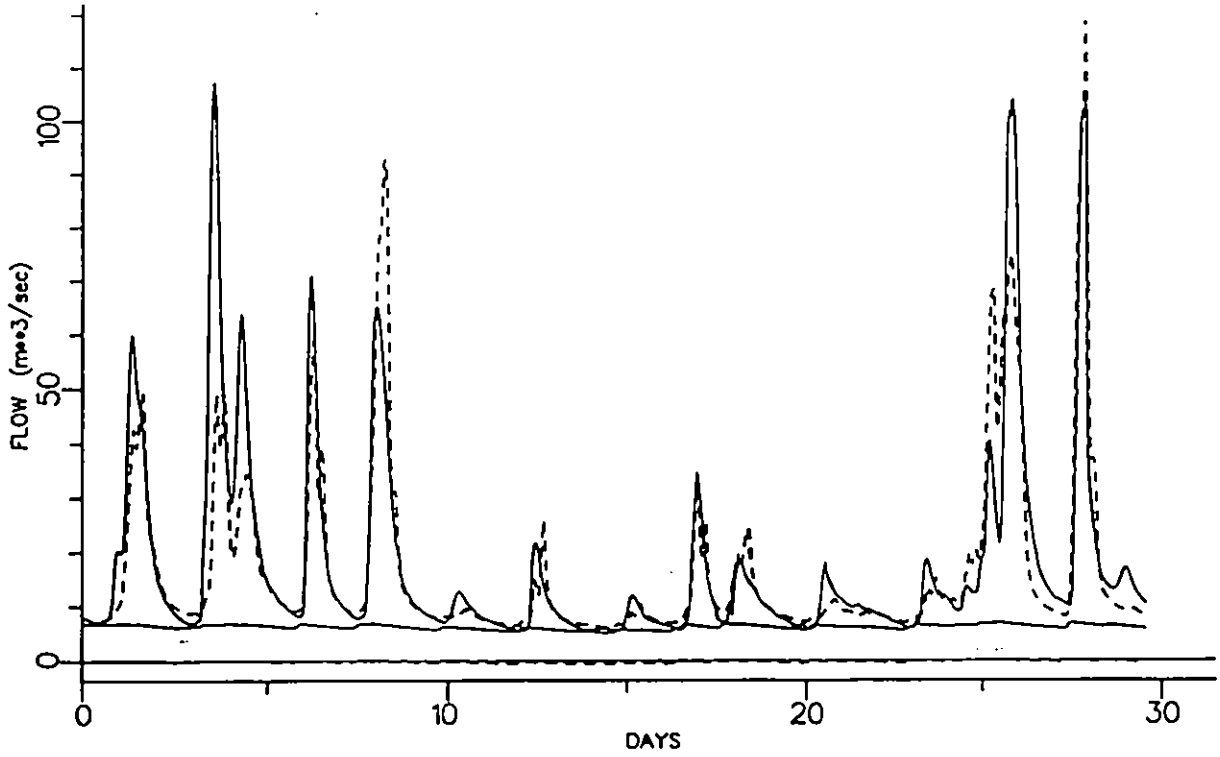

Figure 5.2 Grid-square model results using 2 km grid-square rainfall data from Hameldon Hill radar; River Wyre at St. Michaels, October 1986.

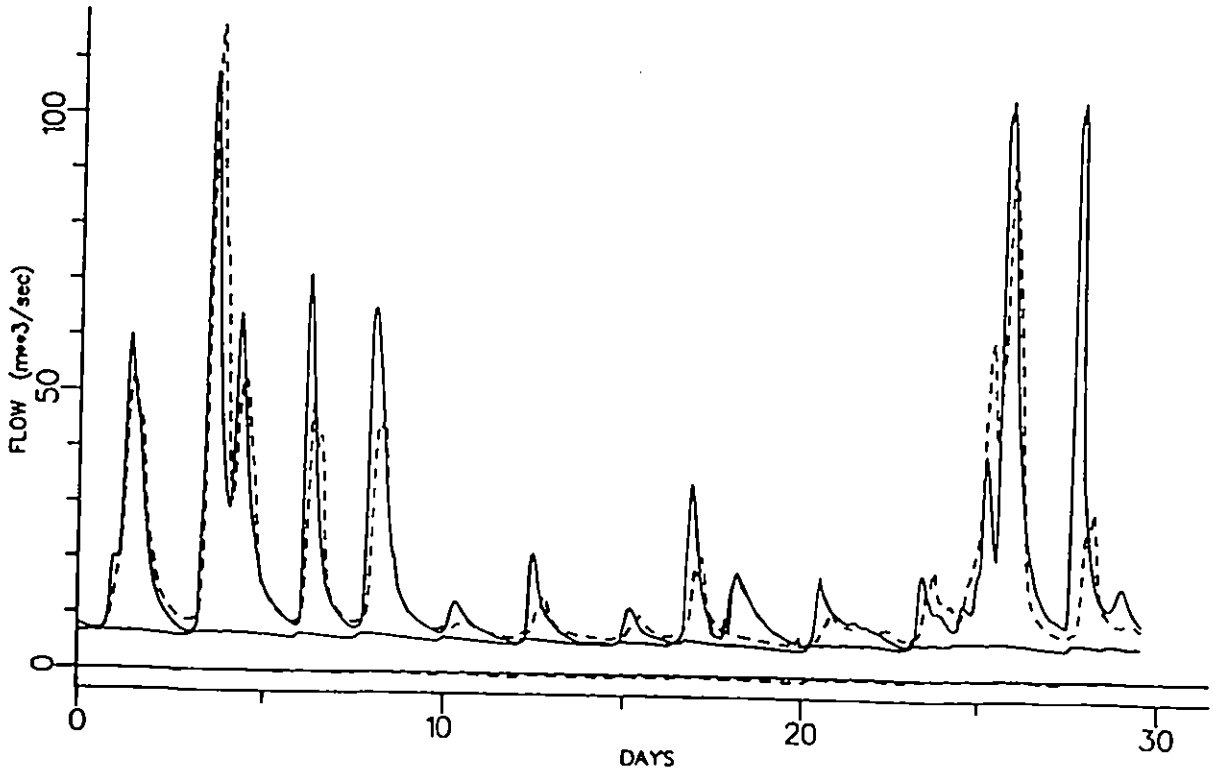

Figure 5.3 Grid-square model results using Abbeystead raingauge data: River Wyre at St. Michaels, October 1986.

6. Design Applications of Weather Radar

6.1 OBJECTIVES

Radar data have been used in a study aiming to provide an improved description of extreme rainfall variations in time and space in upland areas (Stewart, in prep.; Stewart & Reynard, in prep.). The results of the study are particularly relevant to reservoir flood hazard assessment and reservoir safety.

The main region of study was a 10 000 km^2 area centred on the Hameldon Hill radar installation in north-west England. Daily rainfall data from a large number of raingauges within the region were used in the analysis, together with hourly radar-derived rainfall depths for a number of heavy rainfall events. Secondary analyses were carried out using recording raingauge data from the Upper Dee catchment in north Wales.

The analysis of spatial variability focused on the evaluation of statistical areal reduction factors (ARFs) for the Hameldon Hill study region for durations from one hour to eight days and for areas ranging from 25 km^2 to 10,000 km^2 (Stewart, 1989). The event-based radar data were used in a geostatistical study of the spatial structure of extreme rainfall events in north-west England (Stewart & Reynard, 1991).

6.2 RESULTS

Values of ARF were calculated for a range of areal extents for durations from one to eight days using daily raingauge data. The results suggest that ARFs for upland regions are lower than those currently recommended for design, which are assumed to apply throughout the UK. Areal reduction factors were also found to decrease with increasing return period. A new methodology for calculating short-duration ARFs was developed involving the joint use of radar and raingauge data. The methodology was applied to the Hameldon Hill study region and the results are broadly in line those given in the Flood Studies Report (Natural Environment Research Council, 1975) for durations from one to 12 hours (Fig. 6.1). The incompleteness of the radar record was problematic and precluded a thorough analysis of the return period effect at short durations.

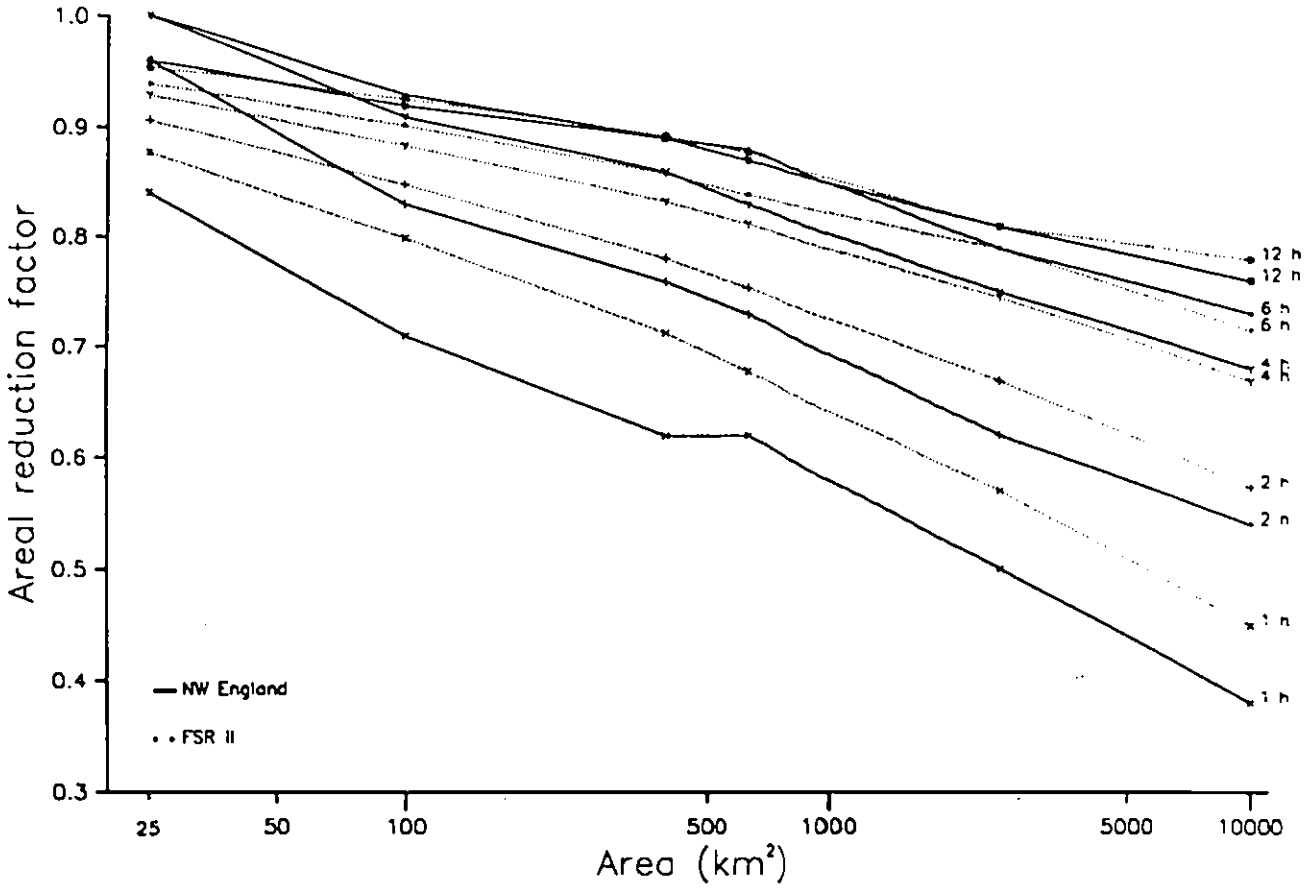

Figure 6.1 Areal reduction factors for north-west England from joint use of radar and raingauge data

A geostatistical analysis of the hourly radar data revealed a high degree of small-scale variability within heavy rainfall events in the study region. It was found to be impossible to characterize rainfall type on the basis of variogram structure, although this conclusion may reflect the resolution of the data. The spatial structure of daily rainfall was found to correspond to that of hourly totals in about half of the rain days studied.

6.3 CONCLUSIONS

Problems of accuracy and the lack of long records limit the usefulness of radar data to design studies and make it necessary to blend the data with information from raingauges. However, the high spatial and temporal resolution of radar data is undoubtedly advantageous in upland areas, where the siting and maintenance of raingauge networks can be difficult.

7. Urban Applications of Weather Radar

7.1 INTRODUCTION

This chapter reports on research work conducted as part of the project by the Water Resources Research Group at the University of Salford. The research has addressed a number of aspects important to the use of weather radar data for urban hydrology.

7.2 RADAR PREPROCESSING

Radar reflectivity data are in their fundamental form represented as continuous voltages. Production of discrete quantitative rainfall values entails quantisation of the analogue signal. In the United Kingdom, two quantisation schemes are utilised resulting in radar data streams having two quite different intensity resolutions.

The highest intensity resolution data are obtained from an eight-bit quantisation scheme. This produces quantitatively precise rainfall estimates across 208 intensity ranges[1], the rainfall intensities for each radar element therefore having any one of 208 values. Precision is related to intensity so that intensities in the range 0 - 2 mm/hr are precise to within $\pm$0.03125 mm/hr; 2 - 8 mm/hr $\pm$0.125 mm/hr; 8 - 32 mm/hr $\pm$0.5 mm/hr; and 32 - 126 mm/hr $\pm$2.0 mm/hr. Eight-bit data are often referred to as quantitative data.

In the second scheme the analogue signal is quantised using eight-bit slicing. This scheme produces data across eight intensity ranges. Because the underlying values from which the display colours are derived are not available (only the upper and lower bounds of the slice ranges) these data are commonly referred to as qualitative or picture quality data. The existence of three-bit data is largely attributable to historical constraints associated with the economic and technical aspects of display device hardware and data transmission. The first radar imaging systems commercially produced in the U.K. were limited to displaying colour-coded radar images with no more than eight colours.

Despite the manifestly lower intensity resolution of three-bit data, and rapid technological developments, radar rainfall data quantised across eight intensity ranges

---

[1] the other 48 bits are used for internal consistency, parity and error checks.

remain the favoured resolution for the UK national network, European (COST) and quantitative precipitation forecast (FRONTIERS) images.

This project has investigated the common assumption that low intensity resolution, three-bit data do not possess sufficient accuracy for quantitative hydrological applications. A key aspect of this work has been the recognition of the concept of information content and its application to the description of basic data characteristics.

Considerable attention has focussed on the used of three-bit radar rainfall data for flood forecasting in rural river catchments (Tilford, 1987; Cluckie, Tilford and Shepherd, 1991). The conclusion being that flood forecasts derived from a three-bit radar rainfall input do not significantly differ from those derived from a high intensity resolution eight-bit rainfall input. Furthermore, the flood forecasting models themselves could be satisfactorily identified and calibrated from three-bit rainfall data sequences.

An explanation is provided by a consideration of the physical processes associated with runoff generation (evapotranspiration, percolation, overland flow etc.). These intermediary processes result in runoff being far less variable and more predictable than the causal rainfall, complex physical interactions introducing a filtering element. Many flow forecasting models simulate this natural low-pass filtering of catchment processes by employing a mathematical convolution process to modulate the rainfall input signal. The research has now been extended to investigate whether these observations are relevant to the urban environment.

The simulation software used is the WASSP-SIM section of the Wallingford Procedure (National Water Council, 1983), a software package which allows an urban drainage network to be mathematically modelled and simulated using either design storms of stated frequency or by actual event data. The package can accommodate either lumped or distributed rainfall input. Procedures have been developed to use eight and three-bit radar rainfall data as an input to the WASSP-SIM package for the simulation of runoff over urban areas.

Within WASSP, the methodology used to compensate for the temporal variation of rainfall across a catchment requires the application of a filter that modifies point rainfall measurements. This allows the portion of the event that has just passed over the catchment, and also that portion which will be over the catchment at the time of the next data item, P_t, to be taken into account.

The equation that describes this filter is:

$$P_t = \mu P_{t-1} + (1 - 2\mu)P_t + P_{t+1}$$

where μ is a function of catchment area and data time increment.

However, the current range of data products available at the level of definition thought necessary (2 km spatial resolution and a time resolution of five minutes), are only available as eight-bit data. Whilst conversion of eight-bit data to a three-bit representation produces obvious differences in the respective rainfall profile, overall

differences between the cumulative rainfall derived from the eight and three-bit rainfall data are generally less than 10%, providing that the rainfall exceeds 5 mm. Figure 7.1 shows an envelope scattergraph of the ratio eight/three bit cumulative rainfall against the eight bit cumulative value for the event. Approximately 15,000 such events were examined to produce the scattergram which for convenience is reproduced as an enclosure graph.

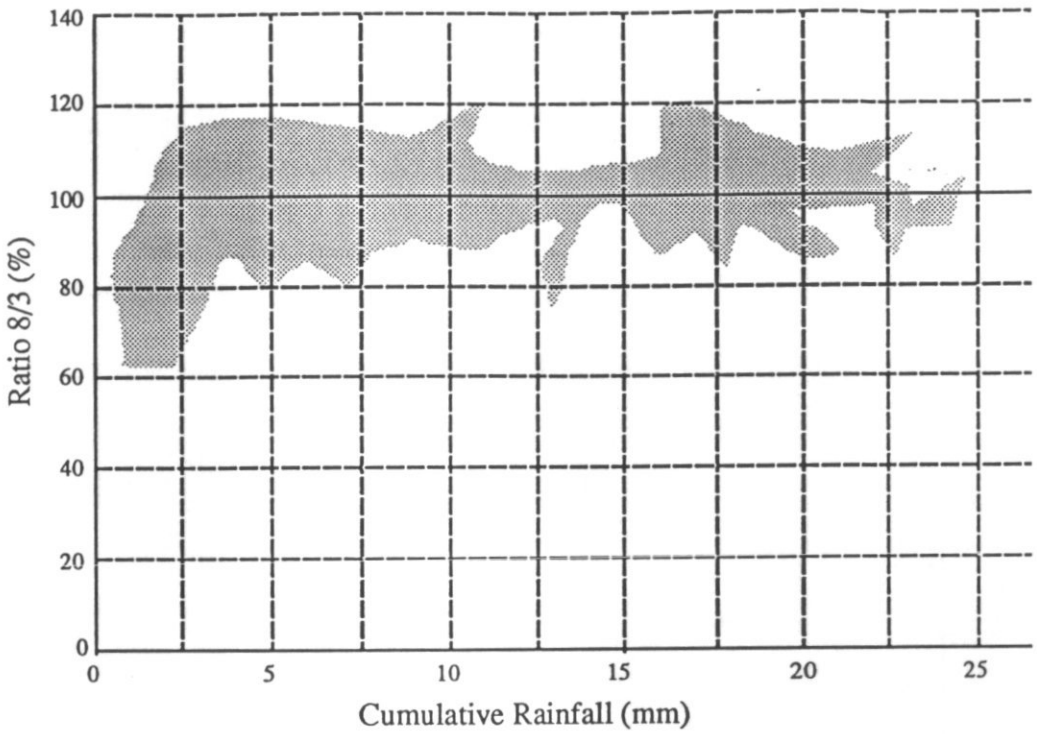

Figure 7.1 Enclosure scattergraph: Conversion error as a function of total rainfall

These profiles (and many others) have been used in conjunction with the WASSP-SIM package. Initial work was carried out using a theoretical, linear pipeline designed using a rational method to ensure adequate capacity. Output hydrographs were plotted at nodes along its length for simulation using both eight-bit and three-bit input data. Examples of the hydrographs are shown in Figure 7.2 and show that the differences are minimal by node G and are probably insignificant some distance before this point. The simulations were extended to an actual surface water network: for the town of St. Hellier in Jersey, Channel Islands. The sample results in Figure 7.3 indicate similar results.

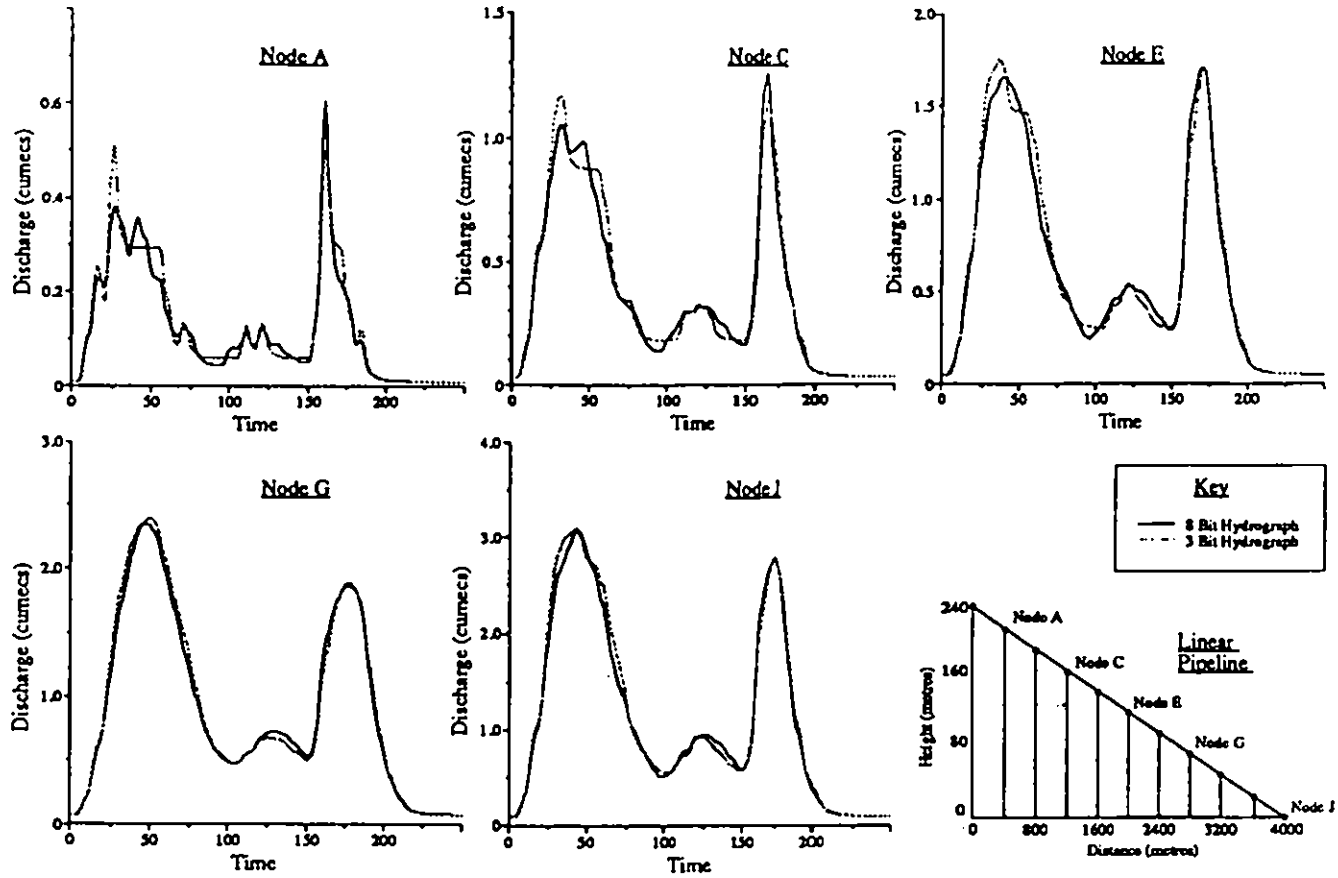

Figure 7.2 Hydrograph simulation for a linear pipeline using eight and three-bit rainfall data

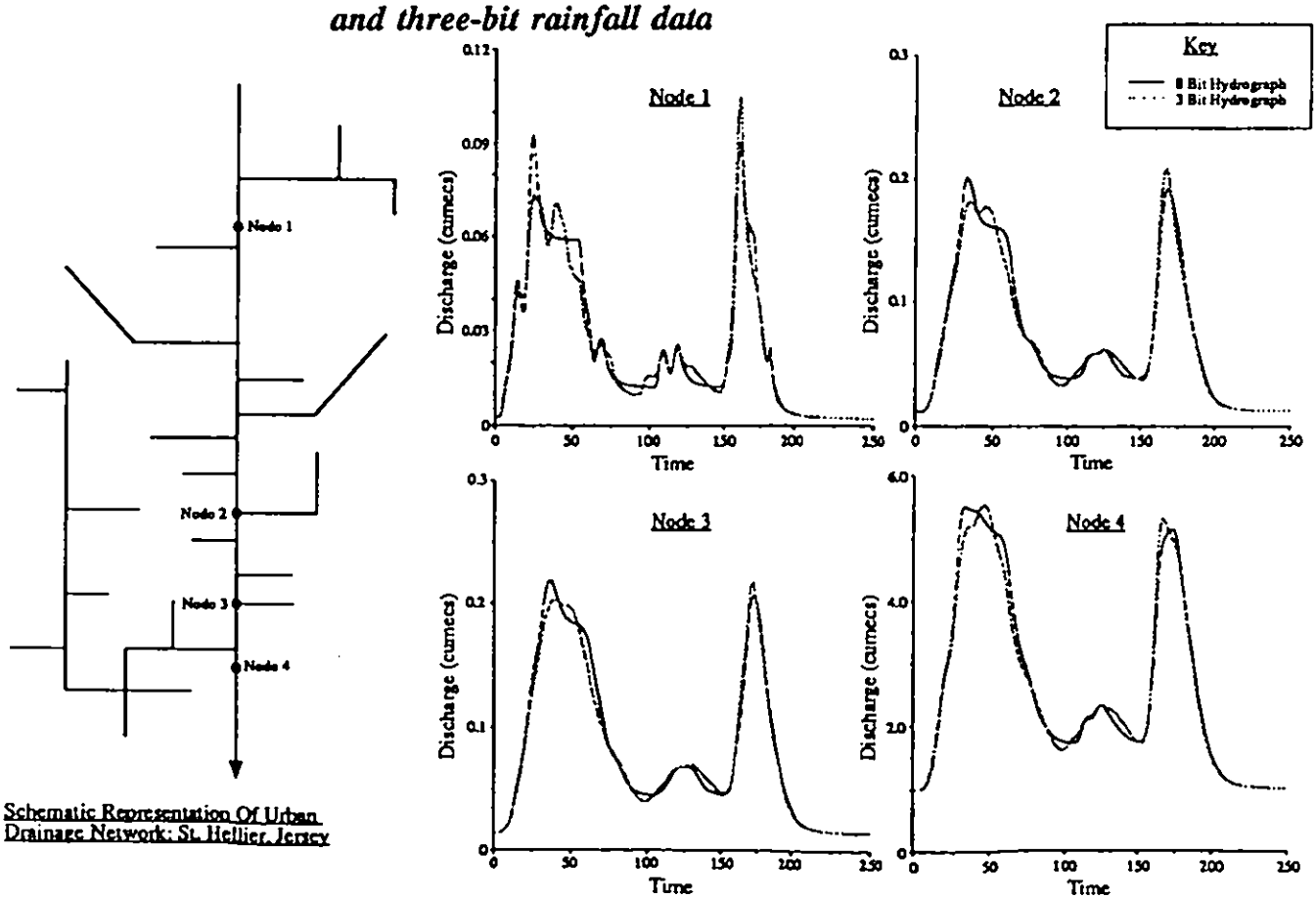

Figure 7.3 Hydrograph simulation for St Hellier urban drainage network

The conclusion appears to be in accordance with the detailed observations drawn earlier in the section regarding the effect of the simulation model on the high frequency component of the input data signal. The size of the urban drainage area directly affects its ability to respond to high frequency input signals and, in many cases of practical relevance, the catchment acts as a low pass filter.

7.3 CALIBRATION

Increasing attention has focussed on the use of sophisticated and powerful two-dimensional interpolation and surface fitting algorithms as a means of improving the accuracy of radar rainfall estimates. The rationale underlying this is that the point accuracy of raingauges can be used in conjunction with the high spatial resolution of the radar data to derive an adjusted rainfall field which portrays the actual rainfall field with higher accuracy than either of the rainfall fields in isolation. An adjustment procedure has been developed incorporating this approach.

The raingauge-based radar rainfall adjustment procedure can be considered as a three phase process:

- computation of assessment factors at each of the raingauge locations.
- two dimensional surface fitting of the scattered assessment factors. This results in a regularly distributed assessment factor field on a grid coincident with the cartesian grid used by the radar (2 km or 5 km).
- node by node multiplication of the unadjusted radar data by the 'mapped' assessment factors to produce an adjusted rainfall field.

Each phase in the process is shown in Figure 7.4.

The following modified form of a simple assessment factor, where the assessment factor is defined to be the ratio of radar rainfall value, R_r, to raingauge rainfall value R_g is used to overcome discontinuities when the gauge rainfall is zero:

$$AF = \frac{R_r + \lambda}{R_g + \rho}$$

Selection of the constants ρ and λ is not straightforward and for simplicity both are set to unity.

It is worth noting that many other definitions of assessment factors can be derived (e.g. Moore, *et al.*, 1991) though the benefits of alternative forms are difficult to assess.

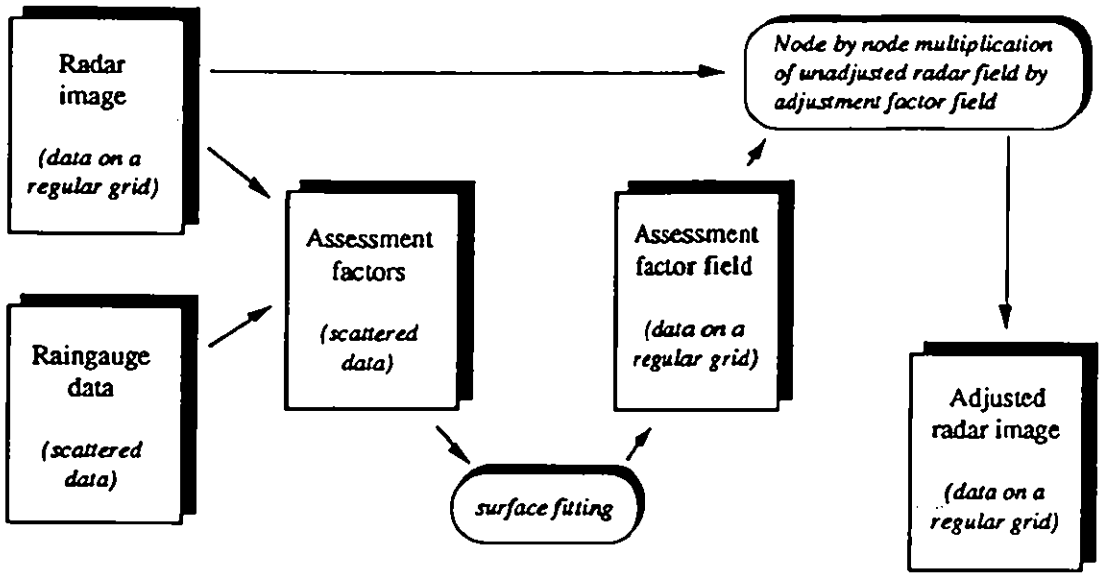

Figure 7.4 Schematic representation of radar rainfall data adjustment incorporating two-dimensional surface fitting of assessment factors

Although the assessment factors can be formed over any time interval (limited only by the temporal resolution of the rainfall data), preliminary studies indicate that a cumulation period of one-hour produces reasonable results and reduces the number of occasions where there is no or minimal rainfall (thereby reducing error in the assessment factor). Upper and lower bound constraints (0.1 and 10.0) are applied to the assessment factors to prevent adjustment from being too radical or unstable in time. AF values greater than 1.0 indicate that the unadjusted radar values will be increased by adjustment (inferring overestimation by the radar), whilst values less than 1.0 indicate that the unadjusted radar values will be reduced by adjustment (inferring underestimation by the radar). A value of exactly 1.0 indicates no change.

A number of two dimensional interpolation and surface fitting algorithms have been investigated. Of these, two interpolation and one surface fitting algorithm are favoured. All the algorithms work with irregularly distributed data. The interpolation algorithm is not explicitly used for radar adjustment but to derive a representation of the spatial rainfall field from the point raingauge data facilitating a visual comparison of the radar and raingauge rainfall fields. The surface fitting routine is used to map the irregularly distributed assessment factors to a regular grid coincident with the cartesian grid of the radar data.

The fundamental problem that any interpolation or surface fitting procedure for data scattered in the plane (such as raingauge rainfall data) addresses is the following (after Renka and Cline, 1984):

'...given a set of nodes (abscissae) (x_i,y_i) arbitrarily distributed in the x-y plane, with corresponding ordinates $z_{i,\ i=1,2,\ldots,M}$, construct a bivariate function $F(x,y)$ which interpolates/fits a surface to, the data values, ie, $F(x_i,y_i)=z_i,\ i=1,2,\ldots,M$...'.

The problem arises in a wide variety of scientific fields in which the data represents observed or computed values of some physical phenomenon. Information usually derives from points whose locations are determined logistically rather than as a result of network optimisation considerations, so that in practice most existing operational raingauge networks can be considered as randomly distributed as regards the observed rainfall process. Regardless of the algorithm used, a satisfactory fit cannot be expected if the number and arrangement of the data points do not adequately represent the character of the underlying relationship. Ideally data points should extend over the whole domain of interest of the independent variable and extrapolation outside the data ranges is unwise.

A smooth interpolatory surface is often desired when a visual impression of the surface is required. The main requirements for an interpolation scheme are (Shepard, 1968):

- the two dimensional interpolation function is to be 'smooth'.
- the interpolated surface must pass exactly through the specified data points.
- the interpolated surface should meet the user's intuitive expectations about the phenomenon under investigation.

Interpolation methods may be either local or global. In a global method the interpolant is dependent on all the data points regardless of their distance from the interpolation point, whereas in a local method, the interpolant does not depend on data points more than a certain distance from the interpolation point. Often a local method is used to avoid prohibitive computation time, although for rainfall, especially localised convective storms, a global method would not be appropriate.

The main constraint applied to interpolation schemes is that the interpolating function passes exactly through each of the data points. This ensures an exact rendition of the rainfall field at the sampled points, though can in the case of rainfall result in a contorted surface. This is because the rainfall process is spatially dynamic (i.e. may be highly localised) and discontinuous. If this constraint is relaxed such that the interpolation function need not fit the given values exactly, trend surface fitting (Krumbein, 1959) may be appropriate. An advantage of this approach is that distortion of the estimated rainfall arising from possible random error in the data (measurement / observation error) may be reduced. Many surface fitting procedures, including the one described, provide user control of the smoothness of fit / closeness of fit balance by way of a smoothness parameter. It should be noted that if the fit is too smooth the signal will be lost (underfit), and if too close the surface may pick up too much noise (overfit).

The instantaneous radar rainfall intensities are averaged at hourly intervals to produce mean rainfall depths for that hour at each grid cell. Likewise the raingauge rainfall

depths are cumulated over the hour for each raingauge. At each raingauge location assessment factors, *AF*, are derived.

Once the assessment factors have been defined for all raingauge locations a bicubic spline surface is fitted. The result is a regular assessment factor field with AF defined for points coincident with the cartesian radar grid. Adjustment of the hourly radar image is then achieved by multiplying each of the unadjusted radar rainfall values by the collocated assessment factor at each point (i,j) in the rectangular adjustment domain $(i_{min},j_{min})*(i_{max},j_{max})$, that is

$$R_{ad}(i,j) = R_{unad}(i,j) \quad AF(i,j), \qquad i = 1,p; \quad j = 1,q \qquad (7.1)$$

where there are p points along the x-axis and q points along the y-axis.

The form of the assessment factor field surface and hence, the adjusted radar data is controlled by the surface smoothness parameter S of the surface fitting algorithm. In addition, S also controls (in addition to the grid mesh size, field complexity and number of data points) the execution speed of the surface fitting algorithm. Preliminary investigations considering computational and estimation considerations have led to the adoption of a single value for the smoothness parameter.

A case study is used to illustrate the adjustment procedure. The event is frontal stratiform with rainfall relatively even across the case study area. Significant amounts of rainfall occurred during the day, the bulk between the period 12:00 and 22:00 GMT. The average raingauge rainfall total for the 66 available gauges is 16 mm (i.e. approximately 1.6 mm/hr) and the low spatial variability of rainfall over the area is indicated by the standard deviation of the gauge measurements of 3 mm. In addition to widespread and heavy rainfall, the event is complicated due the enduring presence of a bright-band. The severity of the bright-band is primarily due to its low height (approximately 500 m), consequently filling the beam at near range when the beam width is relatively small. The event therefore presents a stern test of the adjustment procedure in conditions where the greatest error in radar rainfall estimates can be expected.

Figure 7.5 shows four different images: unadjusted radar rainfall field (a), the corresponding radar image after adjustment (b), the interpolated raingauge rainfall field (d) and the mean assessment factor field (c) applied to the 24 hourly radar rainfall images. All the rainfall fields (i.e. (a), (b) and (d)) are cumulated over the entire available period and are in mm depth units.

There is a striking difference between the unadjusted radar and raingauge derived rainfall fields with significant overestimation by the unadjusted radar data throughout the area, but strongest within 50 km range of the radar. The mean assessment factor field reflects this, having a mean value of less than unity for the day, signifying that the adjustment procedure is on average lowering the unadjusted radar rainfall estimates). The adjusted radar rainfall field more closely resembles the raingauge field, with the worst of the bright-band overestimation removed.

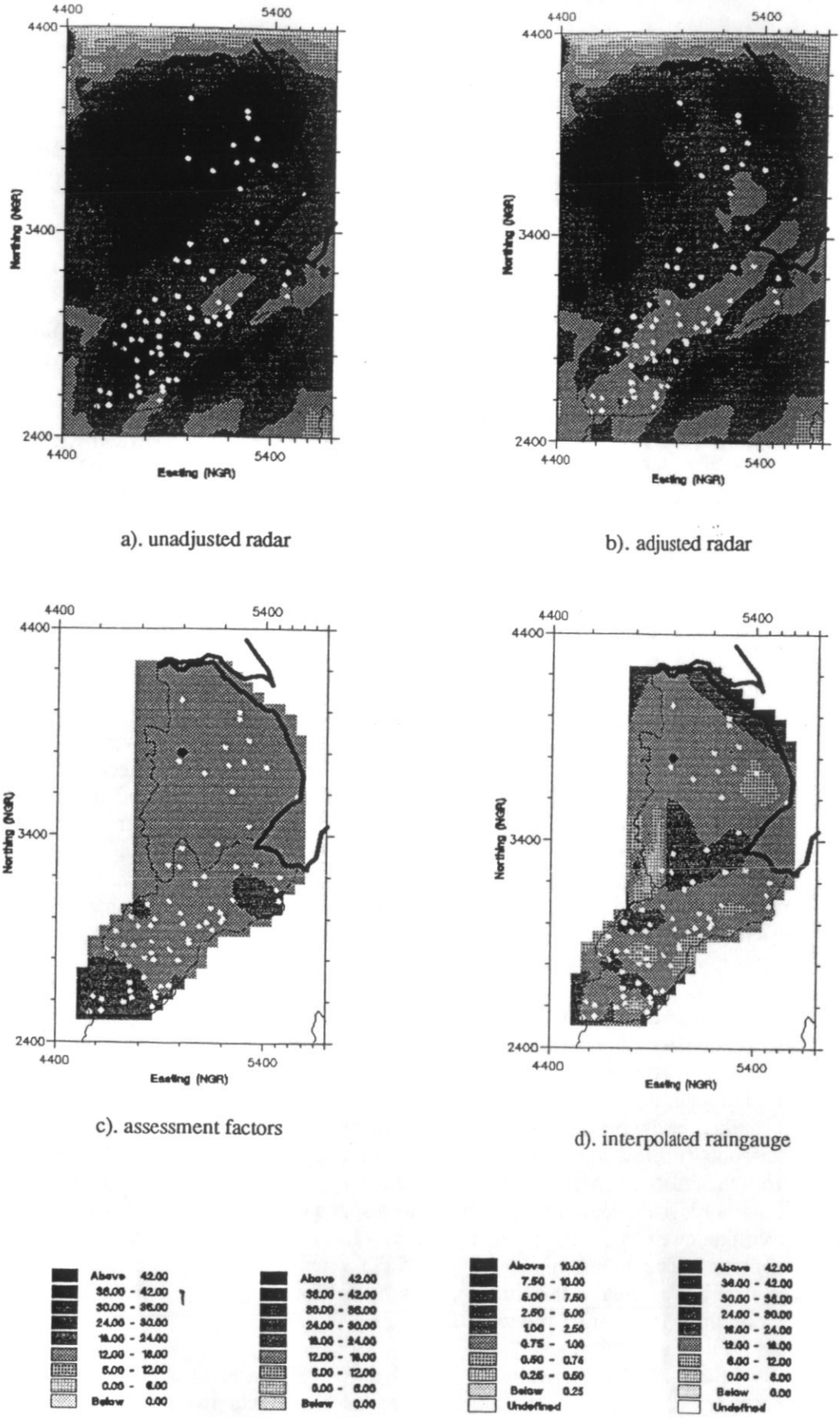

Figure 7.5 Radar adjustment fields, 18 December 1989

7.4 FACTORS INFLUENCING THE RADAR-RAINGAUGE RELATIONSHIP: VERTICAL REFLECTIVITY PROFILES

A number of factors influence the radar-raingauge relationship, a number of which have been discussed previously. This section will concentrate on the vertical reflectivity profile. It is envisaged that an improved knowledge of physical atmospheric processes will lead to an improvement in the quality of quantitative radar rainfall estimates.

In April 1991 a vertically pointing radar was commissioned by the Water Resources Research Group at the Department of Civil Engineering, University of Salford. The radar is an X-band (3 cm, 9,400 MHz) Racal-Decca ship navigation device customised by the McGill Radar Weather Observatory, Montreal, Canada, for meteorological applications. Unlike most hydrometeorological radars, the device does not scan radially but points vertically providing quantitative information on the vertical reflectivity structure of the atmosphere in the form of a height-time image. The ultra-high resolution of the device (2 seconds, 7.5 m vertical) enables the structure of storms to be studied in great detail, from near ground level up to 12 km altitude.

The most significant problem in the UK (and many other countries with a temperate climate) is due to the bright-band layer: a significant increase in reflectivity arising from the melting of solid phase water as it passes through the 0° isotherm (melting layer). Inadequate vertical resolution even quite close to the radar can provide problems for identification and correction since the bright-band layer may be as little as 200-300 m in thickness. Furthermore, the bright-band may fall above or below the radar beam at any particular location (see following paragraph). The presence of a bright-band layer may introduce large errors into precipitation estimation and can result in overestimation of rainfall intensities by up to a factor of ten.

The requirement to use elevated beams to overcome local obstructions and beam occultation introduces a second source of error which arise from the resulting divergence between the beam and the Earth's surface. The problems include: low level precipitation may be missed altogether; low level precipitation enhancement may take place below the beam; low level evaporation may occur; precipitation may drift horizontally below the beam. Since the beam height is primarily a function of range from the radar, the problems become increasingly significant as the range increases. Orographic enhancement may be in the lowest 500 m or so which is invariably below even the lowest beam elevation of the conventional scanning radar. A further source of error is due to incomplete filling of the volume sample of the radar. This is primarily a function of the beamwidth used, and consequently becomes increasingly important as range from the radar increases.

The Salford-McGill Vertically Pointing Radar is being used to address some of the more important problems and shortcomings associated with precipitation observation and quantitative estimation using scanning weather radars. The project has enormous future potential and a wide range of topics is currently being researched. The topics

identified as high priority are: the bright-band layer, orographic effects, and the spatial/temporal variability of the vertical reflectivity profile.

As yet no objective technique has been developed to identify and correct for errors introduced by the bright-band layer in real-time. The VPR is working in conjunction with an existing C-band scanning radar operated by the UK Meteorological Office. The scanning radar provides estimates of average precipitation in a volumetric cell of the order 1 km^3 at a height of typically 2000 m above the ground whilst the VPR will provide 7.5 m resolution time-height profiles at 2 second intervals from 100 m above the ground to well above the height of the scanning radar beam. The additional information provided is invaluable in studying the presence and dynamics of the bright-band layer. In addition orographic effects and other height changes in precipitation can be analysed.

Sufficient experience of the operation of the VPR at several ranges and bearings from the scanning radar will facilitate the development of numerical correction algorithms (meteorological/range/location) to be explicitly computed and incorporated into the real-time scanning radar processing system. The anticipated correction algorithms will incorporate components to correct for the effects not only for bright-band but also for orographic, sampling, beam overshooting, and beam filling effects. Validation of the corrections made to the scanning radar data will be made with reference to a mini-network of real-time telemetering raingauges. The potential for the development of expertise and methods for improved operation of scanning radars is regarded as most significant, particularly in the urban domain where increasing attention is being paid to the development of techniques for the real-time control of urban drainage systems.

This section shows examples of a number of storms observed during the summer of 1991. The examples provide a glimpse of the capability and potential of the radar, and of the analysis and development work currently being pursued at Salford. Figure 7.6 shows height-time reflectivity diagrams for two rainfall events observed. Information is currently being collated from a variety of different sources including synoptic charts, radiosonde data, scanning radar data (Hameldon Hill), and raingauge data from local gauges operated by the National Rivers Authority, North West Region. The diagrams provide a revealing insight into storm structure and dynamics for a range of different storm types:

- a well defined and relatively stable bright-band layer (at 3200 m) within light stratiform rainfall of varying intensity (Figure 7.6(a) - 15th September),

- a classic anvil structure within a stratiform event. Note low bright-band at 800 m, and regions of convection in the upper cloud (Figure 7.6(b) - 3rd June).

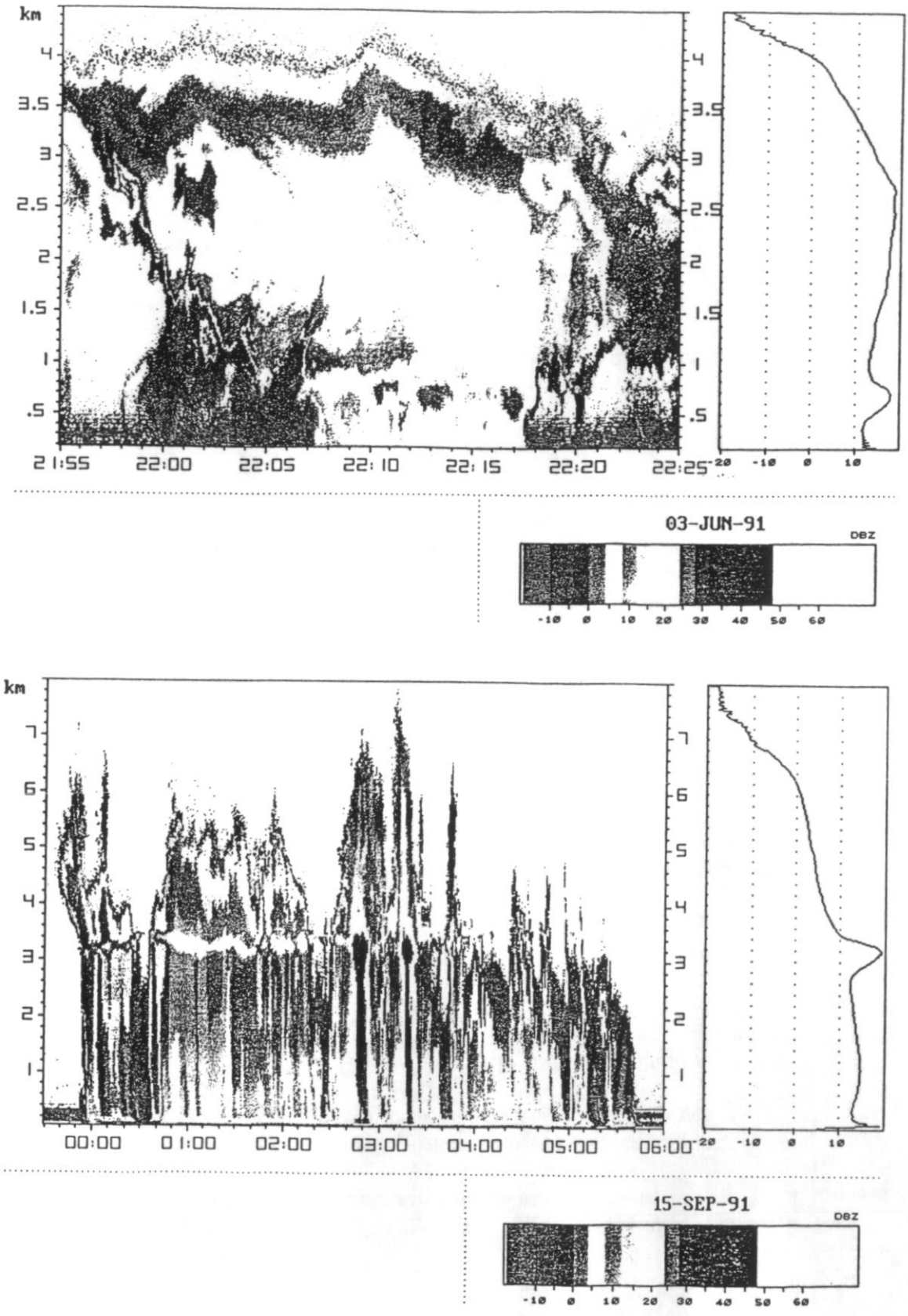

Figure 7.6 Height-time reflectivity diagrams from the Salford-McGill VPR

7.5 URBAN DRAINAGE MODELLING

7.5.1 Influence of Temporal Resolution: 5 minute and 15 minute data.

The influence of temporal resolution was analysed by a simulation of the Bolton drainage system using a variety of rainfall data. Average rainfall amounts were accumulated for the entire duration of the storms for data resolutions of 5, 10, and 15 minutes.

The difference between the 5, 10 and 15 minute rainfall data was not significant. The influence of the temporal data resolutions was minimal with relative deviations of up to 2.8%, but was more significant when comparing peak flows and overflows. At sensitive locations the relative deviations between the peak flows could reach as much as 35%. Generally as the temporal resolution decreases both the deviation and the number of pipe locations indicating large deviations between peak flows increased. The decrease in temporal resolution actually changed the rainfall intensities and the temporal distribution. Hence, if the low temporal resolution data are utilised the peak flow and overflows will be under- or over-estimated at certain sensitive locations within the urban drainage system. The underestimation of peak flows and overflows would bring hazards and overestimation would result in overspending on the design, renewal and rehabilitation of the system.

Five minute data are considered to be the minimum requirement for modelling urban drainage systems, either for off-line design or real-time simulation. If the modelling is limited to large diameter pipes (say, exceeding 1 m diameter), or a catchment with a longer response time than the Bolton system, then lower temporal resolution data may suffice. These aspects will be further clarified by modelling a system with a catchment area of 240km^2 with the benefit of a low cost C-band radar development in the near future.

7.5.2 Influence of Spatial Resolution: 2 km and 5 km data

In their fundamental form radar data are polar. However for ease of use a cartesian conversion is applied by the at-site computer in real-time, the resultant data having spatial resolutions of either 2 km (within 75 km range of the radar) or 5 km (to 210 km). The fall in spatial resolution with range is primarily attributable to beam divergence.

The influence of the spatial resolution on the modelling and simulation of an urban drainage system was in general more significant than the temporal resolution. The relative deviation between the inflows generated from 2 km and 5 km radar rainfall data ranged to 26%, some 10 times the magnitude of the relative deviations between

inflows generated from 5 and 15 minute data for the same storm data. A decrease in the spatial resolution, results in an increase in the deviations between both the peak flows and overflows. This is particularly sensitive at key locations on the pipe network and is primarily due to the spatially distributed nature of the rainfall field.

The results of the analysis suggest that 5km and lumped (i.e. single areal values) are inadequate for urban drainage system modelling and do not possess sufficient information of small scale effects in the rainfall field which are important for many urban drainage systems. The conclusion is necessarily limited to the Bolton drainage system, and is dependent on the system characteristics being indicative of urban systems elsewhere. Further analysis is required on larger urban systems and will form part of planned future work.

7.5.3 Influence of radar wavelength: simulated X-band and C-band rainfall data

The low relative cost and potential portability of X-band radar devices are the two main reasons why radar systems operating at this wavelength are currently being considered for use (primarily France and Germany) in urban hydrology. However, X-band systems are subject to increased levels of interference and attenuation. A detailed investigation has been conducted to compare quantitatively X-band and corresponding C-band radar rainfall data from an urban hydrology perspective. The investigation has focussed on three aspects: rainfall comparisons, flow comparisons, and comparisons of combined sewer overflows. The analysis has been conducted using the the WASSP-SIM package (described in section 7.1) for the Bolton urban drainage network.

Storm rainfall data over Montreal, Canada, as observed by an S-band radar operated by McGill Radar Weather Observatory supported the comparative analysis. Numerical attenuation formulae (below) were applied to the S-band data (S-band can be considered to be a non-attenuating wavelength) to yield simulated rainfall estimates for hypothetical collocated C- and X-band radars.

X-band attenuation: $A = 0.011\ R^{1.5}$

C-band attenuation: $A = 0.0062\ R^{1.0}$

where R is the rainfall rate in mm/hr and A the point attenuation in dBz. Upper bounds on the possible attenuation were set to 6 dBz/km (X-band) and 2 dBz/km (C-band).

The deviation between rainfall measurements obtained from the X-band and C-band data, in terms of the absolute deviation, varies with rainfall rate at the target location, horizontal range and the rainfall blocking along the scanning beam. It has a distinct correlation with the total rainfall over a period so that an increase in total rainfall is always accompanied by an increase in the deviation between the X- and C-band data.

One storm produced as much as 50% less rainfall with X-band data when compared to C-band data. Importantly, the X-band signal is often attenuated below the minimum detectable signal threshold of the radar. The significance of this is that the signal cannot therefore be influenced by any real-time reconstruction or calibration procedure.

The flow deviation was represented by the standard deviation and the peak flow deviation was indicated by the absolute deviation and the relative deviation. The standard deviation showed that the deviation of flow was very minor as a whole but could be very significant for peak flows which are largely rainfall dominated. The deviation of peak flow is more sensitive to pipe location than the other factors. The sewer network was observed to attenuate and smooth the input rainfall signal, producing a low frequency flow response. The impact of high frequency elements within the rainfall measurement is consequently lessened.

The results showed that the correlation coefficients between areal rainfall rate and mean overflow, as well as the absolute deviation of the mean overflow, were very large (0.92 and 0.80 respectively), implying that overflow is proportional to rainfall amounts, i.e. the greater the overflow the larger the absolute deviation. Such a conclusion will hold at least in the case of the Bolton catchment when subjected to the data range used in the study.

From the analysis it was seen that quantitative radar rainfall measurements can be significantly affected by the radar wavelength. The deviations between flows was not significant in general but the peak flows, the lag times and the combined sewer overflows determined by the deviation of rainfall together with many other factors were relatively significant. This would affect the design and the real-time control of urban drainage systems in a very substantial way, and would certainly result in high costs due to the uncertainties in flow estimation, the consequent implications in terms of pollution, over or under design and flooding. The fact that very high intensity rainfall can attenuate an X-band signal to the extent that rainfall is not observed at all is particularly serious since there is no possibility for signal reconstruction procedures to be invoked.

The data are in general prone to difficulty in interpretation at ranges beyond 10 km and very intense convective storms will pose problems even at closer range. Providing that low cost C-band devices can be developed specifically for use in those urban areas that do not have good coverage from existing large scale C-band meteorological network radars, then it is not recommended that X-band scanning radars are seriously considered for widespread exploitation in urban hydrology. The development of overlapping X-band networks may to some extent mitigate against the problems described but remain the subject of future research.

7.6 CONCLUDING COMMENTS AND RECOMMENDATIONS

The work on the development of urban radar technology has advanced to the extent that a number of studies are underway or planned within Europe. The Water Resources Research Group at the University of Salford will be extending their interest into the real-time control of large urban drainage systems as a direct consequence of the research described.

8. Conclusions

The main findings of the research project are summarised below as a set of conclusions under the heading of each section.

Section 2 Radar Preprocessing and Calibration

(1) Routine correction for radar blockage by structures and topography is quite inadequate, and can be very considerably improved by carefully adjusting radar measurements of rainfall totals over long periods to agree with gauge measurements.

(2) Time-variable two-dimensional calibration surfaces for widespread rain using selected calibration gauges are much more effective when applied to radar data improved as in (1), even when using many fewer calibration gauges.

(2) Orographic enhancement of rainfall by the local hills is complex, varies quickly in response to changes in the speed and direction of airflow, and its effect on radar calibration requires careful calibration as in (2).

(4) In widespread rain, agreement between gauge and radar data is significantly improved by including a term in $(\text{range})^{0.25}$, though the exponent varies strongly with meteorological situation. Note that the procedure in (1) also corrects for any consistent range effect.

(5) Extensive periods of widespread precipitation without brightband fit a raingauge:radar rainfall measurement relation of the form $R_g = a R_r^b$ with $a=2$ (SD 0.6) and $b=0.6$ (SD 0.3). Time series of b in prolonged rainfall show apparently coherent variations, with minima near the passage of the surface front.

(6) Time-variable calibration of radar measurements of extensive rainfall is significantly improved when a time series analysis technique based on the Kalman filter is used to marry temporal consistency with white noise.

(7) Radar measurements of convective rainfall can differ very widely from gauge measurements, tending to underestimate heavy falls (especially in the vicinity of strong gradients of echo strength, and at higher beam altitudes) and overestimate light falls.

Section 3 Local radar calibration

(1) Using a multiquadric surface fitting algorithm to combine data from 30 raingauges and a weather radar can improve the accuracy of rainfall measurement, on average, by 22% compared to that obtained using radar alone. This result applies to an area of low relief in the vicinity of London in southern England. The improvement may be as great as 45% in widespread frontal rain; the risk of reducing the accuracy during localised convective storms appears slight using the specially developed surface fitting method.

(2) The practical viability of implementing a local radar calibration procedure has been demonstrated: the Radar Calibration System has been running since 14 March 1989 in support of NRA Thames Region's flood warning service.

Section 4 Local radar rainfall forecasting

(1) The use of radar rainfall images to infer the speed and direction of rainfall field movement and its use in rainfall forecasting has been demonstrated. A simple advection-based model, incorporating a correction to shrink the forecast towards the field average with increasing lead time, performs better than more complex methods incorporating acceleration and intensification components. The pattern of the forecast rainfall deteriorates beyond one hour, and beyond two hours the use of a single radar makes it impossible to forecast the whole of the target rainfall field.

Section 5 Grid-square rainfall runoff model

(1) Use of a digital terrain model, or a contour map, to overcome the problem of overparameterisation of distributed rainfall-runoff has been demonstrated. An assessment of the merits of using distributed radar rainfall in grid-square rainfall runoff models, relative to the use of data from a single raingauge, has been frustrated by blockages affecting the radar measurements of rainfall in the study region.

Section 6 Design applications

(1) The shortness, and problems of accuracy, of existing archives of radar rainfall data limit the usefulness of these data in hydrological design studies. However, a combination of radar and raingauge data has proved useful in assessing short-duration areal reduction factors.

Section 7 Urban applications

(1) Hydrological models in general appear to be relatively robust in relation to the quantisation of the radar signal. 3-bit (8-level) data, providing the numerical allocation process is carefully chosen, appears to contain sufficient information content to allow real-time hydrological modelling to proceed.

(2) The spatial and temporal resolution of quantitative data for use in urban drainage network models was studied and recommendations made regarding the requirements of weather radar use in urban situations.

(3) Detailed development of high density local raingauge adjustment procedures have been successful and are being commissioned and field-tested in two regions. Work on specific urban procedures for both off-line and real-time application over urban catchments have also been developed and are now being deployed.

(4) Fundamental radar characteristics were studied in relation to urban hydrology and recommendations made as to preferred wavelength and implications on quantitative accuracy. C-band devices were considered to be optimal for medium to long range applications (i.e. > 20 km range).

(5) Studies of the vertical reflectivity profile have been initiated in order to improve understanding of vertical storm structure and provide additional information for real-time data adjustment algorithms

References

Section 2:

Archibald, E.J. (1991) An assessment of the quality of Hameldon Hill radar data for quantiative use at longer ranges. Institute of Environmental and Biological Sciences Report, Lancaster University .

Austin, P.M. (1987) Relation between measured radar reflectivity and surface rainfall. Mon. Weather Rev., 115, pp. 1053-70.

Brown, K.R. (1991) The orographic enhancement of rainfall in N.W. England using surface and radar data. Thesis to be submitted for Ph.D., Lancaster University.

Collier, C.G. (1986) Accuracy of rainfall estimates by radar:Part I; calibration by telemetering raingauges. J. Hydrol., 83, pp. 207-23.

Collinge, V.K. (1989a) Weather radar calibration: Final Contract Report to North West Water. Institute of Environmental and Biological Sciences Report, Lancaster University, 49 pp.

Collinge, V.K. (1989b) Weather radar calibration in real time - prospects for improvement. Proc. of International symposium on hydrological applications of weather radar, Salford.

Collinge, V.K. (1990) Relationship between radar-estimated rainfall and raingauge-measured rainfall. Institute of Environmental and Biological Sciences Report, Lancaster University, 52 pp.

Collinge, V.K., Archibald, E.J., Brown, K.R. and Lord, M.E. (1990) Radar observations of the Halifax storm, 19 May 1989. Weather, 45, pp. 345-65.

Hill, F.F., Browning, K.A. and Bader, M.J. (1981) radar and raingauge observations of orographic rainfall over South Wales. Q. J. R. Meteorol. Soc., 107, pp.643-70.

Young, P.C. (1984) Recursive estimation and time-series analysis. Springer-Verlag, Berlin.

Zawadski, I. (1984) Factors affecting the precision of radar measurements of rain. Proc. of 22nd. Conference on Radar Meteorology, Zurich.

Section 3:

Collier, C.G., Larke, P.R. & May, B.R. (1983) A weather radar correction procedure for real-time estimation of surface rainfall. Q.J.R. Meteorol. Soc., 109, 589-608.

Creutin, J.D. & Obled, C. (1982) Objective analysis and mapping techniques for rainfall fields: an objective comparison. Water Resour. Res., 18(2), 413-431.

Gandin, L.S. (1965) Objective analysis of meteorological fields. Leningrad, 1963 (Transl. Israel Programme for Scientific Translation), 242 pp.

Hardy, R.L. (1971) Multiquadric equations of topography and other irregular surfaces. J. Geophys. Res., 76(8), 1905-1915.

Haggett, C.M. (1986) The use of weather radar for flood forecasting in London, Conference of River Engineers (1986), Cranfield 15-17 July, Ministry of Agriculture, Fisheries and Food, 11pp.

Jones, D.A., Gurney, R.J. & O'Connell, P.E. (1979) Network design using optimal estimation procedures, Water Resour. Res., 15(6), 1801-1812.

Lancaster, P. & Šalkhauskas, K. (1986) Curve and Surface Fitting: An Introduction, Academic Press, 280 pp.

Moore, R.J. (1990) Use of meteorological data and information in hydrological forecasting. In: A. Price-Budgen (ed.), 'Using Meteorological Information and Products', 377-396, Ellis Horwood.

Moore, R.J., Watson, B.C., Jones, D.A., Black, K.B., Haggett, C., Crees, M. & Richards, C. (1989a) Towards an improved system for weather radar calibration and rainfall forecasting using raingauge data from a regional telemetry system. New Directions for Surface Water Modelling, IAHS Publ. No. 181, 13-21.

Moore, R.J., Watson, B.C., Jones, D.A. & Black, K.B. (1989b) London weather radar local calibration study: final report. Contract report prepared for the National Rivers Authority Thames Region, 85pp, September 1989, Institute of Hydrology.

Moore, R.J., Watson, B.C., Jones, D.A. & Black, K.B. (1991) Local recalibration of weather radar. In: I.D. Cluckie and C.G. Collier (eds), Hydrological Applications of Weather Radar, 65-73, Ellis Horwood.

Section 4:

Collinge, V.K. (1989) Investment in Weather Radar by the UK Water Industry, Weather Radar and the Water Industry, British Hydrological Society Occasional Paper No. 2, 1-13, Institute of Hydrology.

Conway, B.J. & Browning, K.A. (1988) Weather forecasting by interactive analysis of radar and satellite imagery. Phil. Trans. R. Soc. Lond., Ser. A, 324, 299-315.

Moore, R.J., Hotchkiss, D.S., Jones, D.A., and Black, K.B. 1991. London Weather Radar Local Rainfall Forecasting Study: Final Report. Contract Report to the National Rivers Authority Thames Region, Institute of Hydrology, September 1991, 124 pp.

Section 5:

Anderl, B., Attmannspacher, W. and Schultz, G. A., 1976. Accuracy of Reservoir Inflow Forecasts Based on Radar Rainfall Measurements. Water Resources Research, 12(2), 217-223.

Chander, S. and Fattorelli, S., 1991. Adaptive grid-square based geometrically distributed flood forecasting model. In: Cluckie, I. D. and Collier, C. (Eds.), Hydrological Applications of Weather Radar, 424-439, Ellis Horwood.

Moore, R. J., 1991. Use of Meteorological Data and Information in Hydrological Forecasting. In: A. Price-Budgen (Ed.), Using Meteorological Information and Products, 377-396, Ellis Horwood.

Moore, R. J., 1992. Grid-square rainfall-runoff modelling for the Wyre catchment in North-West England. Proceedings of the CEC Workshop: Urban/rural application of weather radar for flow forecasting, 3-4 December 1990, Dept. of Hydrology, Soil Physics and Hydraulics, University of Wageningen, The Netherlands, 4pp.

Moore, R.J., Hotchkiss, D.S., Jones, D.A. & Black, K.B. (1991) London Weather Radar Local Rainfall Forecasting Study: Final Report, Contract report to the National Rives Authority, Thames Region, September 1991.

Section 6:

Natural Environment Research Council (1975) *Flood Studies Report* (five volumes). NERC, London.

Pilgrim, D. H., Cordery, I. & French, R. (1969) Temporal patterns of design rainfall for Sydney. *Civ. Eng. Trans. I. E. Aust.*, CE11(1), 9-14.

Stewart, E. J. (1989) Areal reduction factors for design storm construction: joint use of raingauge and radar data. *IAHS Publ. No. 181* (Proc. Symp. on New Directions in Surface Water Modeling, Baltimore, May 1989), 31-40.

Stewart, E. J. (in prep.) Spatial variations of extreme rainfall events in upland areas. *Contract report to the Department of the Environment.*

Stewart, E. J. & Reynard, N. S. (1991) Variability of heavy rainfall events in north-west England: an analysis of spatial structure. In: *Hydrological Applications of Weather Radar* (ed. by I. D. Cluckie & C. G. Collier), 192-202. Ellis Horwood, Chichester.

Stewart, E. J. & Reynard, N. S. (in prep.) Temporal variations of extreme rainfall events in upland areas. *Contract report to the Department of the Environment.*

Section 7:

NWC (1983) Report to the Working Group on National Weather Radar Coverage, National Water Council/Meteorological Office.

Cluckie, I.D., Tilford, K.A. & Shepherd, G.W. (1991) Radar rainfall quantisation and its influence on rainfall-runoff models. In: I.D. Cluckie and C.G. Collier (eds), *Hydrological Applications of Weather Radar*, Ellis Horwood.

Tilford, K.A. (1987) Real-time flood forecasting using low intensity resolution radar rainfall data, M.Sc. Thesis, Department of Civil Engineering, University of Birmingham, unpublished, 78 pp (including appendices).

Moore, R.J., Watson, B.C., Jones, D.A. & Black, K.B. (1991) Local recalibration of weather radar data. In: I.D. Cluckie and C.G. Collier (eds), *Hydrological Applications of Weather Radar*, Ellis Horwood.

Renka, R.L. & Cline, A.K. (1984) A triangle-based C1 interpolation method, *Rocky Mountain J. Math.*, 14, 223-227.

Shepard, D. (1968) A two-dimensional interpolation function for irregularly spaced data. *Proc. 23rd Nat. Conf. ACM, Brandon/Systems Press Inc.*, Princeton, 517-523.

Krumbein, W.C. (1959) Trend surface analysis of contour-type maps with irregular control point spacing, *J. Geoph. Res.*, 64, 823-834.